ALTERATIONS IN THE MOLECULAR PROPERTIES OF NEURAL STEM CELLS FROM AGED BRAINS AND BRAIN TUMORS

A THESIS SUBMITTED TO

THE GRADUATE SCHOOL OF ENGINEERING AND SCIENCE

OF BILKENT UNIVERSITY

IN PARTIAL FULFILLMENT OF THE REQUIREMENTS FOR

THE DEGREE OF

MASTER OF SCIENCE

IN

NEUROSCIENCE

By

Özge Pelin Burhan

June 2017

ALTERATIONS IN THE MOLECULAR PROPERTIES OF NEURAL STEM CELLS

FROM AGED BRAINS AND BRAIN TUMORS

By Özge Pelin Burhan

June 2017

We certify that we have read this thesis and that in our opinion it is fully adequate, in scope and in quality, as a thesis for the degree of Master of Science.

Michelle Marie Adams (Advisor)

Gözde Akar

Ayşe Begüm Tekinay

Approved for the Graduate School of Engineering and Science

Ezhan Karaşan Director of the Graduate School

ABSTRACT

ALTERATIONS IN THE MOLECULAR PROPERTIES OF NEURAL STEM CELLS FROM AGED BRAINS AND BRAIN TUMORS

Özge Pelin Burhan

M.Sc. in Neuroscience

Advisor: Michelle Marie Adams

June 2017

It is known that new neuron formation in the brain continues throughout the life of an organism. In the adult human brain, it was proven that neurogenesis in the hippocampus is higher than expected, almost 700 new neurons are formed in a day. The formation of new neurons is supported by the stem cell subpopulation in the brain. With learning and the formation of new memories, the neuron production increases. However, changes in the cognitive abilities with advancing age are thought to be caused by the functional and molecular alterations in the stem cell populations. Molecular changes in neural stem cells throughout aging were found to be deterrents of the increased risk of cancer with age, such as tumor suppressor mechanisms. However, the activation and overlap of tumor suppressing mechanisms result in senescence in stem cells that have accumulated oncogenic mutations, which causes the stem cell pool exhaustion. It is thought that cancer cells acquire stem cell-like properties in order to have the unlimited proliferation and self-renewal properties, which are characteristics of both healthy and cancer stem cells. Neural cancer stem cells have the ability to produce glial and neural cells, like normal stem cells. The cancer stem cell subpopulations are implicated in the growth of tumor tissues. Hence, it is important to identify and characterize cancer stem cells and make a distinction between cancer and non-cancer stem cells. In this project, this issue was addressed by studying the marker expressions of brain tumor tissues obtained from humans, which confirmed that the cancer cells do express stem cell and progenitor cell markers, such as Sox2 and Vimentin. The presence of mature neurons was also established by the mature neuronal marker NeuN. In order to determine whether these stem cells may be different in young and old subjects, a study was also carried out in young and old zebrafish neural stem cells in order to identify the expression differences between the groups. The presence of proliferating stem cells and differentiated cells were identified in cell culture. This analysis of neural stem cells in old and young zebrafish revealed 18 differentially-expressed genes. The results indicated a higher

differentiation rate in old zebrafish stem cells, which may be due to the increased loss of neural cells in the old zebrafish brain.

The development of markers that could be widely used for the diagnosis of cancer and the identification of cell types is important. For reliable diagnosis and identification of cancer cells, multiple cellular markers are used. Hence the distinction of cell types based on light scattering differences would speed up the process of diagnosis, and the elimination of marker used for the distinction of cell types would be beneficial. The final project mentioned in this thesis involves the analysis of C6 (rat glioma) cell line for scattering properties and cell cycle arrest. A general method for definition of a scatter data interval for C6 cells in different stages was developed and can be applied to other cell types and diseases. These studies show that the proliferation and stem cell markers' expressions differ between cancer and healthy stem cells, and the expression of neuroprotective genes is differentially upregulated in old zebrafish neural stem cells compared to the young. This data could contribute to the knowledge on normal and cancer stem cell expression differences, as well as how age affects the expression, and supply information required for the development of a cancer stem cell identification and targeting methods.

Keywords: Neural stem cells, cancer stem cells, zebrafish, glioma, RNA-seq analysis, flow cytometry

ÖZET

YAŞLI BEYİNDEN VE BEYİN TÜMÖRLERİNDEN ELDE EDİLEN NÖRAL KÖK HÜCRELERİN MOLEKÜLER ÖZELLİKLERİNDEKİ DEĞİŞİKLİKLER

Özge Pelin Burhan

Nörobilim Lisansüstü Programı, Yüksek Lisans

Tez Danışmanı: Michelle Adams

Haziran 2017

Canlılarda yeni nöron oluşumu, nörogenez, her yaşta devam etmektedir. Yapılan araştırmalarda, yetişkin insan beyninin hipokampüs bölgesinde her gün yaklaşık 700 yeni nöron oluştuğu gözlemlenmiştir. Yeni nöron oluşumu beyindeki nöral kök hücre populasyonu tarafından desteklenmektedir. Öğrenme ve yeni anı oluşumunun nörogenezi arttırdığı gözlenmiştir. Yaşlı beyinde nörogenez devam etmesine rağmen bilişsel fonksiyonlar azalmaktadır. Buna yaşlanmayla birlikte kök hücre populasyonlarındaki moleküler ve fonksiyonel değişimlerin sebep olduğu düşünülmektedir. Yaşlı organizmalarda kök hücrelerin DNA tamir mekanizmalarının işlevselliğinin azaldığı ve bu sebeple kanser oluşumunu tetikleyici mutasyonların zamanla arttığı gözlemlenmiştir. Kanser oluşumunu engellemek için yaşlı organizmaların kök hücrelerinde tümör baskılayıcı yolakların aktifleştiği ve tumor oluşturma riski taşıyan kök hücrelerin hücre döngüsünü askıya aldığı belirlenmiştir. Yaşlanma sebebiyle kök hücrelerin senesens fazına girmesi replike olabilecek kök hücre sayısının azalmasına sebep olmaktadır. Kök hücrelere benzer özelliklere sahip olan kanser kök hücreleri de kendilerini replike edebilir, yenileyebilir ve normal kök hücreler gibi başkalaşmış hücreler oluşturabilirler. Kanser kök hücrelerinin tümör dokularında bulunduğu, tümörün büyümesi ve yayılmasına sebep olduğu düşünülmektedir. Bu sebeple, kanser kök hücre ve normal kök hücre ayrımı ve karakterizasyonu önem taşımaktadır. Bu projede normal ve kanser kök hücre işaretçi ifadelerini ve farklılıklarını inceledik. Vimentin ve Sox2 gibi kök hücre ve öncü hücre işaretçilerini ifade eden hücreleri, tümör içerisindeki kök hücre populasyonunun varlığını gösterdi. Beyin kök hücrelerindeki yaşa bağlı farklılıkların incelenmesi için genç ve yaşlı zebrabalığı beyinlerinden kök hücre elde edilmiş, immün boyamalarda elde edilen hücrelerin bölünme, başkalaşma ve kök hücre işaretçileri taşıdığı görülmüştür. Ayrıca yapılan RNA sekans analizlerinde genç ve yaşlı

balık nöral kök hücreleri arasında farklı seviyelerde ifade edilen 18 gen saptanmıştır. Bu sonuçlar yaşlı balıklar kök hücrelerinde daha yüksek başkalaşım hızı olduğunu ve genç balıklara göree fazla ifade edilen genlerin nöron koruyucu özellikleri olduğunu göstermektedir.

Kullanılan hücre işaretçilerinin sadece kanser veya normal kök hücrelerde bulunmadığı gözlemlenmiştir. Sadece kanser kök hücrelerinde bulunan işaretçilerinin araştırılması hem diagnoz hem de hücre hedefli tedavi geliştirilebilmesi için önemlidir. Şu an kanser hücrelerinin karakterizasyonu için hastadan doku alınmakta ve birden çok hücresel işaretçi ifadesine bakılmakta ve bu işlemler diagnoz sürecini yavaşlatmaktadır. Bu tez çalışmasında bahsedilen son projede hücrelerin bilgisayar modellemesi için C6 (sıçan glioma) hücre hattının hücre döngüsünün farklı fazlarında akış sitometrisi cihazıyla ışık saçılım ölçümleri yapılmıştır. Bu çalışmada sağlıklı ve hastalıklı hücre tiplerine belirli ışık saçılım araklıklarının atanması hedeflenmiştir. Her hücre tipine özgü ışık saçılım değerlerinin belirlenmesiyle, hücre karakterizasyonu için işaretçi kullanımının gerekliliğinin ortadan kaldırılması amaçlanmıştır. Bu çalışmalar sonucunda kanser ve normal kök hücrelerinin bölünme, kök hücre ve başkalaşmış hücre işaretçilerini farklı olarak ifade ettikleri, RNA sekans analizindeyse yaşlı nöral kök hücrelerinin daha çok var olan olgun nöronları korumaya yönelik genleri ifade ettikleri gözlemlenmiştir. Bu veriler, normal ve kanserli kök hücre gen ifade farklılıklarının tanımlanması, yaşın kök hücrelerde gen ifadesine etkilerinin anlaşılması ve bir kanser kök hücre tanımlama ve hedefleme yöntemlerinin geliştirilmesi için gerekli bilgi sağlanmasına katkıda bulunabilir.

Anahtar sözcükler: Nöral kök hücreler, kanser kök hücreleri, zebrabalığı, glioma, RNA sekans analizi, akış sitometrisi

Acknowledgement

I would first like to express my profound gratitude to my thesis advisor Assoc. Prof Michelle M. Adams and to Dr. Ayca Arslan-Ergul for their guidance, support and allowing me to work on intriguing projects that would build and expand my skills and knowledge. Without their encouragement, I would not have stepped into the field of bioinformatics.

I would like to thank Prof. Gozde Bozdagi Akar and Assoc. Prof. Ayse Begum Tekinay for their kindness on accepting to take part in my thesis committee. I am thankful to Assoc. Prof. Tekinay for also allowing me to use the flow cytometer in her lab.

I consider myself very fortunate to be a part of the lab that has become a second family. Elif Tugce Karoglu, Esra Senol, Naz Serifoglu, Melek Umay Tuz-Sasik, Begun Erbaba, and Narin Ilgim Ardic, I am thankful for their support and friendship.

I would like to thank Tekinay lab members, Gokhan Gunay, Canelif Yilmaz and Idil Uyan for their help.

I would also like to thank Furkan Akdemir for his patience, support and understanding. Without his help, the computational analyses in my thesis could not have been done.

I am thankful to my dear friends Irem Sozen, Yaprak Besik and Elcin Kinikli, Goksemin Fatma Sengul for their love, help and support.

Finally, I would like to express my profound gratitude to my family for providing me with unconditional love, support and encouragement. I could not have written the thesis without their help. Thank you.

I would like to dedicate my thesis to Poki and Abab.

The projects mentioned in chapters 2 and 3 were supported by The Scientific And Technological Research Council of Turkey with grant number 114S548. The reagents used in the last project mentioned in Chapter 4 was bought from the budget of Communications and Spectrum Management Research Center (ISYAM).

Contents

1 INTRODUCTION 1

1.1 Neurogenesis 1

1.2 Stem Cells 3

1.3 Stem Cells, Cancer and Aging 4

1.4 Cell Markers 5

2 Stem Cell Isolation from Human Tumor Samples 7

2.1 INTRODUCTION 7

2.2 METHODS 11

2.2.1 Handling and Storage of Tumor Tissue 11

2.2.2 Stem Cell Extraction 11

2.2.3 Maintaining and Passaging of the Cells 12

2.2.4 BrdU treatments 12

2.2.5 Senescence Detection with Beta-Galactosidase Staining 12

2.2.6 Immunocytochemistry 14

2.3 RESULTS and DISCUSSION 15

2.4 CONCLUSION 22

3 Stem Cell Isolation from Old and Young Zebrafish Brains and RNA Expression Analysis 23

3.1 INTRODUCTION 23

3.2 METHODS 26

3.2.1 Dissection and Stem Cell isolation 26

3.2.2 Slide Coating 27

3.2.3 BrdU Treatment 27

3.2.4 Immunocytochemistry 27
3.2.5 Total RNA isolation from cultured neural stem cells 28
3.2.6 RNA-Seq Methods 29
3.3 RESULTS and DISCUSSION 35
3.3.1 RNA-Seq Analysis 35
3.3.2 Immunocytochemistry 46
3.4 CONCLUSION 48
4 Cell Cycle Arrest and Flow Cytometry Analysis of C6 Cells 49
4.1 INTRODUCTION 49
4.2 METHODS 52
4.3 RESULTS 55
4.3.1 Flow Cytometry 55
4.3.2 Microscopy 58
4.4 CONCLUSION 59
5 Conclusions and Future Perspectives 60
Bibliography 63
Appendix A 74
Appendix B 75
Appendix C 76
Appendix D 77

List of Figures

Figure 1: Immunostaining results of OE4-P2 cells 16

Figure 2: Immunostaining results of OE4-P2 cells 17

Figure 3: Immunostaining results of OE6-P4 and OE7-P1 cells 18

Figure 4: Immunostaining results of OE7-P1 cells 19

Figure 5: Immunostaining results of OE4-P5 cells 19

Figure 6: Immunostaining results of OE4-P5 cells 20

Figure 7: Immunostaining results of OE4-P5 cells 20

Figure 8: Immunostaining results of OE7-P1 cells 21

Figure 9: Color coding of the sample command lines. 30

Figure 10: Depiction of the Tuxedo protocol 31

Figure 11: Command line sample for bowtie2 tool. 32

Figure 12: Command line sample for tophat2 tool 32

Figure 13: Command line sample for cufflinks tool. 33

Figure 14: command line sample for cuffmerge tool 33

Figure 15: command line sample for Cuffquant tool. 34

Figure 16: command line sample for cuffdiff tool. 34

Figure 17: Heat map of genes upregulated in old zebrafish neural stem cells 36

Figure 18: Ugt8 expression difference graph 38

Figure 19: fam101b expression difference graph 39

Figure 20: Cx47.1 expression difference graph 40

Figure 21: Crlf1a expression difference graph. 41

Figure 22: C7 expression difference graph. 42

Figure 23: si:ch211-181d7.3 expression difference graph 44

Figure 24: Immunostaining result of old zebrafish neural stem cells. 46

Figure 25: Immunostaining results of old zebrafish neural stem cells. 47

Figure 26: Immunostaining results of old zebrafish neural stem cells. 47

Figure 27: Depiction of flow cytometer. 51

Figure 28: C6 cells' forward vs. side scatter and count vs. PI graph, no nocodazole treatment. 55

Figure 29: Forward and side scatter graph and count vs. PI graph of the 0.1 μg/ml nocodazole-treated C6 cells. 55

Figure 30: Forward and side scatter graph and count vs. PI graph of the 0.25 μg/ml nocodazole-treated C6 cells 56

Figure 31: Forward and side scatter graph and count vs. PI graph of the 0.5 μg/ml nocodazole-treated C6 cells. 56

Figure 32: Forward and side scatter graph and count vs. PI graph of the 1 μg/ml nocodazole-treated C6 cells. 57

Figure 33: C6 cells after 24 hours of 0.25 μg/ml nocodazole treatment. 58

Figure 34: C6 cells with no nocodazole treatment. 58

List of Tables

Table 1: 1 M NaH2PO4 solution recipe. 13

Table 2: 1 M Na2HPO4 solution recipe. 13

Table 3: 40 mg/ml X-Gal recipe . 13

Table 4: 100 mM K-ferricyanide solution recipe. 13

Table 5: 100 mM K-ferrocyanide solution recipe. 13

Table 6: 100 mM MgCl2 solution recipe. 13

Table 7: 2 M NaCl solution recipe. 13

Table 8: 200 mM Citric Acid recipe . 13

Table 9: Na-P buffer recipe. 14

Table 10: SAβG solution recipe. 14

Table 11: Antibody dilutions used. 15

Table 12: Antibody dilutions used. 28

Table 13: gene_exp.diff file obtained from cuffdiff. 35

Table 14: gene_exp.diff file after the genes after 0 FPKM were values omitted. 36

CHAPTER 1

INTRODUCTION

1.1 Neurogenesis

Neurogenesis is the birth of neurons in the brain. Until recently, it was thought that the brain was not able to produce new neurons. It is now known that new neurons are born in some regions of the brain [1-2]. Hippocampus is a region that neurogenesis occurs even after old age, and it is one of the regions underlying learning and memory abilities [3]. There are studies conducted on the rodent hippocampus focusing especially on learning and memory. In the late 90's, Gould *et al.* presented evidence on new neurons being born in the hippocampus and that the new neurons were associated with learning and memory formation [4]. Late-onset Alzheimer's disease, dementia and the decrease in learning and performing cognitive tasks point to an error in the mechanism of neurogenesis, as one contributing factor. Though it is known that cellular changes throughout the process of aging are responsible for the decline in cognitive abilities, scientists have not arrived at a definite judgment. The evidence suggests that changes in the cellular processes mostly affect cognitive abilities, instead of neuron death [5].

Subpopulations of neural stem cells in the lateral ventricles of the brain give rise to neuroblasts which migrate to the olfactory bulb. This serves the purpose of odor discrimination and new odor memory formation. Another region of the human brain where neurogenesis occurs is the striatum, by tracing the iododeoxyuridine (IdU) carrying neurons of the cancer patients who received IdU treatment. The presence of radioactive uridine positive neurons indicated that the treatment receiving patients were also forming new neurons which were traced to the striatum. Although the functional purpose of the striatal neurogenesis is unknown, the fact that it is less observed in mice than rabbits and monkeys, and increases through evolutionary steps, suggests

that it serves the cognitive flexibility. Frisen *et al.* has shown that the neurogenesis in the adult human hippocampus is crucial for forming new memories and cognitive abilities [6]. In 2014 it was proven that neurogenesis takes place not only in the hippocampus but also in the subventricular zone (SVZ) of the lateral ventricle and the subgranular zone of the dentate gyrus [7]. Another study was done on 71 mammalian species and has shown that the hippocampal neurogenesis and its occurrence frequency varies among species. The neurogenesis rate of the aquatic mammals was found to be the lowest of all, not humans [8].

In cellular aging research, it is important to identify the proliferating and senescent cells. A commonly used method for the identification of proliferating cells is bromodeoxy uridine (BrdU) labeling. BrdU has a thymidine-like structure. Thymidine is incorporated into DNA during regular replication activities. If BrdU, which is structurally similar to thymidine, is added externally, it is incorporated into the DNA. In every cycle of DNA replication, more and more BrdU would be added into the DNA. The BrdU molecules in the nucleus can be visualized by specialized antibodies. This enables the detection of cells that are in the DNA replication stage [9]. BrdU screening experiments comparing 3 and 20 months old mice showed that there is a decrease in neurogenesis in the hippocampal dentate subgranular, up to 90%, and in the subventricular regions of old mice, up to 50% [10]. In the same study, after fibroblast growth factor (FGF)-2 and Heparin-binding EGF-like growth factor (HB-EGF) treatment, neuronal regeneration of old mice increased up to the levels that are seen in young mice; which shows that the aging process is reversible. In another experiment involving electron microscopy and 2 hour period of BrdU marking, it was reported that the stem cells which give rise to new neurons in adult mouse brain are located in the subventricular region and neuron regeneration is impaired with age [11]. Influencing the neurogenesis process by external means and observing the newly arisen neurons have been a topic of interest among researchers. Inhibiting cortico-

steroid levels in old animals, insulin-like growth factor (IGF)-I infusion and even exposing animals to a rich environment have been shown to induce neurogenesis [12].

1.2 Stem Cells

Stem cells are grouped in three: Totipotent stem cells, which can give rise to an entire organism; pluripotent stem cells that are capable of giving rise to every cell of the organism, but not the organism itself, multipotent stem cells are can give rise to the every type of cell of the organ it originates from. Adult neural stem cells are multipotent stem cells that can give rise to neurons, glia, and oligodendrocytes [13-14].

Stem cells continue their presence in most of the mammalian tissues throughout the organisms' life and provide cell-renewal in the case of tissue damage and diseases. It was found that stem cells' function decrease as the organisms age. Stem cells proliferate quickly during the fetal development in order to support organism growth. Throughout the organism's young-adulthood, growth rate (proliferation of the stem cells) in the mammalian tissues decrease and most of the stem cells are inactive (quiescent) during this period, while active stem cells divide to maintain homeostasis of the tissue. In adult rats, it was shown that the proliferation rate of the granular progenitor cells in the hippocampus decreases significantly and neural stem cells obtained from old mice (24-26 months) had formed 50% fewer neurospheres compared to stem cells obtained from young mice (2-4 months) [15-16].

Adult neural stem cells can be maintained in cell culture since they keep proliferating in the presence of epidermal growth factor (EGF) and fibroblast growth factor (FGF). Neurospheres can be formed in cell culture and can be differentiated into neurons, astrocytes, and oligodendrocytes [17]. Use of defined neural inducers, co-use of TGF and BMP inhibitors - double SMAD inhibition have been shown to accelerate neural induction. Pluripotent stem cells

can be differentiated into dopaminergic, striatal, and glial cells, which can be used for studying potential treatments for Parkinson's, Huntington's, and myelin disorders, respectively [18].

1.3 Stem Cells, Cancer and Aging

The quantity of stem cells and their ability to self-renew may not decline with aging, but their capability of making new cells (progenitor and mature, differentiated cells) declines. Self-renewal of the stem cells presents a danger for the organism because the accumulation of DNA damage leads to malignant tissue formation. In older organisms, stem cells increase the expression of tumor suppressor genes and will eventually lead to cellular senescence [19]. Stem cells increasing the expression of tumor suppressor genes and other differences in the regulatory mechanisms of the stem cells suggest the presence of a developmental programming. The stem cells with DNA damage, if not repaired, can pass on to the daughter cells and accumulate. In order to prevent tumor formation, when mutations are detected in stem cells, tumor suppressor mechanisms engage (senescence or apoptosis) and arrest the cell cycle or dispose of the mutant stem cells. The malignant potential of the stem cells and the presence of tumor suppressing mechanisms may be contributing to the aging of the organism by the elimination or inactivation of stem cells. However, the increase in the incidence throughout aging is beyond dispute [20].

Stem cells in the healthy and neoplastic tissue are able to self-renew, and long cellular life causes mutations to accumulate and increase the risk of neoplasia and solid tumor formation. To cure cancer patients, the cancer cells should be eliminated, and the chances of chemotherapy to work decreases as the age of the patient advances, which also causes the stem cells' functionality to decrease. Thus, the characteristics of stem cells that have acquired mutagenic accumulation should be thoroughly studied and a distinction should be made between healthy stem cells and cancer stem cells [21].

1.4 Cell Markers

While normal stem cells have phenotypes that are almost identical to each other and easier to identify, cancer stem cells are complex, different from one tumor to another, and appear to be affected by neoplastic transformation. Single–cell sequencing provided the identification of the different subpopulations of human breast cancer tissue and the opportunity to find out which of the subpopulation is the dominant and metastatic [22]. It should not be overlooked that many phenotypic markers, which allow stem cells to be grouped and isolated, may not be necessary for the functional integrity of stem cells [20]. CD34 is expressed in hematopoietic stem cells and progenitors, and endothelial cells. CD38 is expressed in hematopoietic cells, skeletal muscle, heart muscle and adult prostate cells. Both CD38 and CD44 are involved in the regulation of cell adhesion. CD38 is also involved in cell signaling as an ectoenzyme. CD38 and CD34 are cancer stem cell markers together in hematological cell tumors. In healthy tissue, leukocytes, epithelial, endothelial and mesenchymal cells express CD44. CD44 is also responsible for cell adhesion and migration, as well as cell signaling in healthy tissues. However, it can be used as a cancer stem cell marker for stem cells isolated from breast, colon, gastric, liver and pancreatic tumors. CD24 is expressed in B cells, epithelial cells, and granulocytes, and it is a marker for breast and pancreatic tumor stem cells. CD133 is expressed in the healthy fetal neural and renal stem cells and endothelial stem and progenitor cells. The function of CD133 is not fully understood but it is a cancer stem cell marker for brain, colon, lung, prostate, liver and ovarian tumors. ALDH is another marker that can be found in breast colon and liver tumors with CD133. Astrocytomas, GI tumors, gliomas lung and thyroid cancer stem cells can be distinguished from other stem cells by Hoechst 33342 exclusion [23]. The accurate identification and characterization of cancer cells for diagnosis requires the use of multiple markers. This causes the diagnosis procedure to spread to a long period of time. Hence, the elimination of markers for the identification of cancer cells would save time.

The aim of this thesis work was to isolate stem cells from human brain tumor samples, characterize the stem cells, as well as to identify the age-related gene expression differences in zebrafish brain stem cells and translate the findings into humans. To the last aim was to develop a method for the identification of cancer cells in the bloodstream for the detection of solid tumors.

CHAPTER 2

Stem Cell Isolation from Human Tumor Samples

2.1 INTRODUCTION

Until the presence of neurogenesis in the central nervous system was proven, it was thought that brain tumors emerged from the dedifferentiation of mature brain cells as a result of cancer-causing genetic modifications. With the new understanding of adult neural stem cells, it became clear that tumors arose from the stem cells that adopted cancer characteristics.

The stem cell theory of cancer states that within a population of cancer cells, only some cells (cancer stem cells) are capable of proliferating and sustaining cancer. cancer stem cells are similar to healthy stem cells that renew and divide to provide homeostasis and survival of a tissue. Hence, cancer cells that are not stem cells cannot cause cancer to spread to other parts of the body, they can only contribute to the mass growth of the tumor. Cancer stem cells have the ability to spread through the organism causing metastases and can also contribute to the relapse of cancer after treatment. Many anti-cancer therapies are used for their ability to shrink the size of the tumor. However, this only targets the mature cancer cells. The remaining cancer stem cell population is able to generate a new tumor. Thus, cancer stem cells should be targeted in anti-cancer therapies [24]. Stem cells are capable of proliferating and producing more stem cells. Stem cells can either divide symmetrically and produce two daughter stem cells or divide asymmetrically and produce one daughter stem cell, which maintains the stem cell reserves at a certain level. The commonly used stem cell identification methods are serial transplantation and *in situ* labeling. It is difficult to distinguish tumor stem cells from healthy stem cells. For a stem cell to be classified as a tumor stem cell; the xenograft model it forms should have the

original tumor characteristics and some of the daughter cells should be able to proliferate without forming single cell tumor clones [25-26].

It was found that, CD133+ cell subpopulation had stem cell characteristics in human brain tumors. Xenograft experiments have shown that the CD133+ brain tumor fraction can initiate tumors in the mouse, and only this fraction of the tumor could initiate tumors. When only 100 of these cells were transplanted, serially transplantable tumors with the original tumors' characteristics were formed. It was also observed that about ten thousand of the CD133- cells did not develop tumors. CD133+ cells were purified with magnetic beads and transplanted into the frontal lobe of the 6-week-old mouse. In CD133+ xenografts, double staining of CD133 and glial fibrillary acidic protein (GFAP) suggests that tumor cells that have differentiated and undifferentiated cells coexist in the transplanted tumors. In addition, CD133+ cells may also give rise to CD133- tumor cells [22].

In addition to the mutations that induced the formation of the original tumor, mutations occur throughout the metastasis. This causes the metastatic clones to be heterogeneous. It is difficult to identify which mutations support tumor growth and which will cause the formation of metastatic clones. A nuclear receptor, TLX is found in the neural stem cells and has been associated with the stem cells' and tumor stem cells' self-renewal abilities. Using GFP as a reporter gene fused to the nuclear receptor tailless (Tlx) promoter sequence, Tlx+ cells were found to be silent in primary tumors. With lineage-testing experiments, Tlx+ cells have been shown to be able to regenerate themselves and produce Tlx- cells. This suggests that Tlx+ cells are brain tumor stem cells (BTC) [27].

Advanced genomic sequencing experiments have shown that cancer in a single patient is a heterogeneous mix, composed of genetically distinct subclones [28]. Non-genetic factors create a hierarchical organization of tumor tissues that serve the long-term clonal upkeep of the neoplasm with the support of a cancer stem cell subpopulation that is capable of self-renewal.

Cancer stem cells are found to be resistant to many therapies. The tumor microenvironment is also determinative of cellular functions. Gene expressions specific to cancer stem cells and normal stem cells carry prognostic value for many patients [29]. CD34 and CD38 are used as indicators of human tumor stem cells in acute myeloid leukemia disease. The ability to initiate leukemia is only seen in CD34 + CD38-clones. CD44 + CD24-clones have also been shown to be able to maintain breast cancer clones in the mouse. Each clone harbors cells in different mixes depending on their stem cell characteristics or proliferating ability. Some cells in the mix are in the quiescent state. This serves the functional diversity of the clone.

A recent study showed that silent tumor stem cells survived temozolomide (a chemotherapeutic agent) treatment and turned into a rapidly growing cell population [30]. This study has provided evidence that cancer stem cells exhibit chemotherapy resistance and cytotoxic treatments targeting only dividing cells should be supplemented with therapies targeting quiescent cells. One team, with a 16,000-component library, examined the components that can kill epithelial-mesenchymal transition (EMT) induced cancer stem cells [31]. This study showed that besides paclitaxel, the salinomycin drug could also reduce the tumor seeding ability by a factor of 100. Similar studies have been done for glioblastoma, ovary cancer, breast cancer, and acute myeloid leukemia (AML).

Zhu *et al*, have made double transgenic mice, by activating Ras with the p53 tumor suppressor gene and by combining the mutations of the neurofibromatosis type 1 (Nf1) gene, which increases astrocytoma formation in humans [32]. With the elimination of tumor suppressor genes, activation of oncogenes such as Ras and Akt in neuronal precursor cells has been shown to increase tumor formation [33]. It has also been shown that excessive production of platelet growth factor-beta (PDGFb) in nestin-positive precursor cells or GFAP+ astrocytes enhances glioma formation [34]. Inhibition of the CDKN2A locus in which INK4a and ARF tumor suppressors are present and high expression of the EGF receptor (EGFR) cause mature

astrocytes to form glioma-like lesions after being transplanted into the skull [34]. Genetic subclones should be isolated in order to study cancer stem cells. One method, suggested by Kreso *et al*., is the transplantation of cells in clonal doses. For solid tumors, it is important to select from different regions of the tumor [23].

Recently, Tomasetti and Vogelstein have reported that replication-associated stem cell mutations explain the relationship between lifetime cancer risk and the number of stem cell divisions in tissues [35]. Telomeric shortening may increase the clonal dominance of mutant stem cells during tissue aging. Telomeres in critical shortness induce loss of chromosomal stability and heterozygosity in yeast. In telomerase knockout mice, unstable chromosomal intestinal stem cells on intestinal epithelium accumulated in the absence of p53, which was the first experimental proof that telomere dysfunction draws a response from p53-dependent mechanisms that prevents tissue loss by the extermination of unstable stem cells [36]. Endogenous expression of telomerase, when combined with damage to DNA repair mechanisms, result in genetically unstable cells, which is a characteristic of human aging [37-38]. Reprogramming mature somatic cells and making them pluripotent is a powerful tool for modeling human diseases. However, the reversal of cellular aging during reprogramming produces induced pluripotent cell (iPSC) which causes problems in modeling for age-related diseases [39].

The aim of this project was to isolate stem cells from human brain tumors obtained from patients and characterize the cells by looking at differential marker expressions. Moreover, differences between tumor types and how the age of the patients potentially affects tumor stem cell marker expression were investigated. Information obtained from this work might provide potential biomarker targets for future drug therapies.

2.2 METHODS

2.2.1 Handling and Storage of Tumor Tissue

Tissue storage solution (130-100-008, Miltenyi Biotec) was given in 50 ml falcons to the brain surgeons at Ankara Atatürk Training and Research Hospital. The tissues were put into the storage solutions immediately after the surgery and kept at 4^{o}C. The tissue samples were transferred to UNAM, Bilkent University in an organ cooler with ice. The tissue-containing falcons were put into hood after 70% ethanol disinfection and the remaining portions of the protocol were carried out in a sterile environment to avoid contamination. Ethics permission granted by Ankara University Ethics Committee (11.11.2015) (See Appendix A for a copy of the ethics permission).

2.2.2 Stem Cell Extraction

In order to culture the cells from the tumor tissue, a brain tumor dissociation kit (130-095-939, Miltenyi Biotec) was used. First, the tissues were weighed and cut it into small pieces with a scalpel, then the pieces were washed with HBSS (without Calcium and Magnesium, BE10-543F, Lonza) and transferred into a 15 ml falcon. The samples were centrifuged at 1000 RPM for 2 minutes and the supernatant was discarded. The reagents of the kit were added according to the instructions and incubated in the solution for 15 minutes at 37 ^{o}C under slow and continuous rotation. The samples were further dissociated with the help of fire-polished Pasteur pipettes. After incubation and mechanic dissociation, the cell suspension was run through a 70 nm strainer. The sample was centrifuged again at 1000 RPM for 10 minutes and the pellet was resuspended in cell culture medium containing 500 ml DMEM:F12 (1:1) (11330-032, Gibco), 5 ml Penicillin-Streptomycin (15140-122, Gibco), and 50 ml fetal bovine serum (10270, Gibco).

2.2.3 Maintaining and Passaging of the Cells

The cell culture medium was changed every 3 days, and after the cells had reached 80% confluency, the cells were passaged by washing with PBS (L0615-500, Biowest) twice, then detaching cells with 0.25% Trypsin-EDTA (25200-056, Gibco) at 37 ^{o}C for 5 minutes. To deactivate trypsin, FBS containing cell culture medium was added and the cells were plated in a new cell culture flask in 1:3 dilution. The remaining of the solution was centrifuged at 2000 RPM for 5 minutes and the pellet was stored for protein and nucleic acid isolation.

2.2.4 BrdU treatments

Bromodeoxyuridine (5-bromo-2-deoxyuridine) is a synthetic thymidine analog and is used for the detection of newly synthesized DNA in the proliferating cells [40]. First, a stock solution of 10 mg/ml BrdU (B5002, Sigma) was prepared. One sterile cover slide was placed in each well of a 6-well plate and the cells were plated on the cover slips. The cells were treated with BrdU (1% in complete cell culture medium) and incubated at 37 ^{o}C for 24 hours. Prior to immunostaining procedures, the BrdU-containing medium was aspirated and the wells were washed with phosphate buffered saline (L0615-500, Biowest) twice.

2.2.5 Senescence Detection with Beta-Galactosidase Staining

β-galactosidase staining (SaβG) is a common method for the detection of senescent cells. The method is based on the identification of increased lysosomal β-galactosidase enzyme activity. Cells, under normal conditions, produce the β-galactosidase enzyme in the lysosome. However, in senescent cells lysosomal mass is increased, thus the senescence-associated β-galactosidase can be visualized as a blue stain [41]. The solution used for the assay are described in Tables 1 to 10.

1 M NaH_2PO_4	(stored at 4°C)
	4.8 g NaH_2PO_4
	40 ml dd H_2O

Table 1: 1 M NaH_2PO_4 solution recipe

1 M Na_2HPO_4	(heated up to 40 °C when dissolving)
	7.12 g Na_2HPO_4
	40 ml dd H_2O

Table 2: 1 M Na_2HPO_4 solution recipe

40mg/ml of X-gal	for stock solution
	0.2 g of X-gal
	5 ml dimethyl formamide
	for use in the β-gal assay
	40 mg/ml stock solution in DMSO

Table 3:40 mg/ml X-Gal recipe

100 mM K-ferricyanide	
	0.658 g K-ferricyanide
	20 ml ddH_2O

Table 4: 100 mM K-ferricyanide solution recipe

100 mM K-ferrocyanide	
	0.844 g K-ferrocyanide
	20 ml ddH_2O

Table 5: 100 mM K-ferrocyanide solution recipe

100 mM $MgCl_2$	
	0.406 g of $MgCl_2$
	20 ml ddH_2O

Table 6: 100 mM $MgCl_2$ solution recipe

2 M NaCl	
	2.34 g NaCl
	20 ml ddH_2O

Table 7: 2 M NaCl solution recipe

200 mM Citric Acid	
	2.85 g trisodium citrate
	40 ml ddH_2O
	Adjust pH to 6 with HCl

Table 8: 200 mM Citric Acid recipe

Na-P Buffer	
	10.2 ml 1 M Na_2HPO_4
	29.8 ml 1 M NaH_2PO_4
	adjust pH to 6 with NaH_2PO_4

Table 9: Na-P buffer recipe

SAβG solution	
	2.4 ml 200 mM citric acid
	2.4 ml Na-P buffer
	600 µl Ferricyanide
	600 µl Ferrocyanide
	900 µl 2 M NaCl
	240 µl 100 mM $MgCl_2$
	300 µl X-Gal

Table 10: SAβG solution recipe

Cells were fixed for 15 minutes with cold fixation buffer (FB001, Life Technologies), and incubated in the SaβG solution described in Table 10 for 3 hours at room temperature. Then washed twice with 1X phosphate buffered saline (14040133, Gibco). The assay was followed by the immunocytochemistry protocol described next.

2.2.6 Immunocytochemistry

After BrdU treatment and/or Saβg assay, the cells were washed with PBS twice, then they were fixed in ice-cold methanol for 10 minutes. The methanol was washed away with PBS, then 2N HCl was added to the wells dropwise and kept at 37 ^{o}C for 30 minutes, to permeabilize the cells. HCl was aspirated and the cells were washed with borate buffer (1.9 g Borax in 50 ml PBS) to inactivate HCl. This step was followed by PBS wash. The cells were blocked in goat serum (Sigma) for 30 minutes at room temperature, then were incubated with primary antibody at room temperature for an hour. Anti-NeuN(ab177487, Abcam), neuronal marker, anti-PCNA (ab29, Abcam), proliferation marker, anti-BrdU (5292S, Cell Signaling Technologies), proliferation marker, anti-Sox2 (ab97959, Abcam), neural stem cell marker, anti-TAU

(ab64193, Abcam), neuron marker, were the primary antibodies used. The antibodies were diluted in blocking buffer (dilutions are shown in Table 11). The cells were washed in 0.5% PBS-T 5 times in half an hour on shaker. Secondary antibody incubation was for 50 minutes at room temperature (1:1000 diluted in PBS-T both Alexa 488 and 555), and again the cells were washed with PBS-T 5 times in half an hour.

The cells were either incubated with fluorochrome-conjugated or HRP conjugated secondary antibodies. HRP conjugated antibodies, Goat anti-mouse HRP (ab97023, Abcam) and Rabbit anti-goat HRP (ab97100, Abcam) were diluted 1:1000 in PBS-Tween and the cells were incubated for 50 minutes at room temperature. After 30 minutes wash in PBS-T, the cells were treated with DAB chromogen kit (ab64238, Abcam), 1 drop of DAB chromogen was added into 1.5 ml of DAB substrate and the solution was added onto the cells and kept in dark for 10 minutes. The cells were washed with PBS-T once and mounted with ProLong Gold Antifade (P36930, Life Technologies).

Antibody	Dilutions
anti-Neun	1/250
anti-PCNA	1/500
anti-BrdU	1/500
anti-TAU	1/20
anti-Sox2	1/500

Table 11: antibody dilutions used

2.3 RESULTS and DISCUSSION

Not all information was available regarding the patients and each patient was given an "OE#" id. The sample from OE6 was a craniopharyngioma obtained from a 64-year old patient. Craniopharyngiomas are non-malignant tumors that usually form above the pituitary gland. The sample from OE7 was a meningioma, which is a benign intracranial tumor, obtained from a 21

years-old patient. Meningiomas occur in the membrane that covers the brain and the spinal cord. Benign brain tumors can be life-threatening based on its location and size. Thus, the tumor samples that were used came from both young and old patients and were both solid and neoplastic tumors. The immunostaining results are shown in Figures 1 to 8. The presence of BrdU and PCNA signals indicate that the tumors were a mix of both proliferating cells and newly generated cells. NeuN and TAU are mature neuron markers and Sox2 expression is required for the self-renewal and proliferation properties of the stem cells. The absence of Sox2 signaling indicates differentiation of the cells. OE4-P2 cells were passaged 2 times after stem cell isolation protocol. The information about the patient OE4 was withheld.

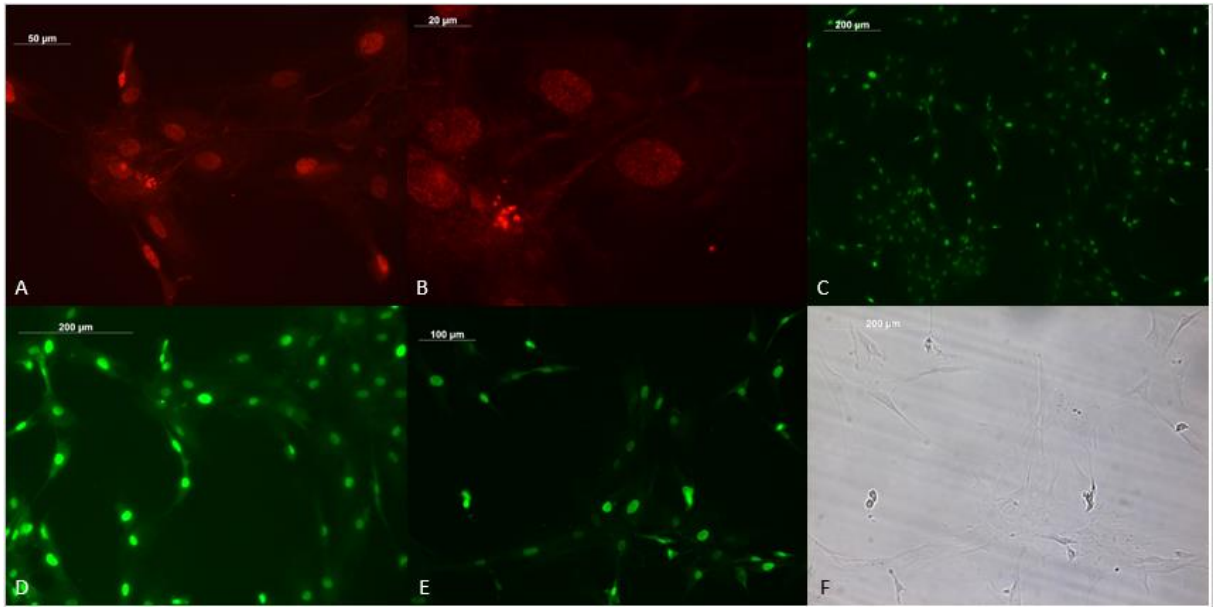

Figure 1: OE4-P2 cells, immunocytochemistry results after stem cell isolation protocol from tumor cells was performed. (a) NeuN staining, scale bar= 50 µm, (b) NeuN staining, same area as (a) with higher magnification, scale bar=20 µm, (c) PCNA staining, scale bar= 200 µm, (d) PCNA staining, same area as (c) with higher magnification, scale bar= 200 µm, (e) PCNA staining, scale bar PCNA staining, scale bar= 100 µm and (f) bright field visualization of the cells in area (e), scale bar= 200 µm.

Due to the absence of epidermal (EGF) or fibroblast (FGF) growth factor, the stem cells differentiated into neurons (Fig. 1a, b). As NeuN labels mature neurons, and BrdU staining indicates newly generated cells, the presence of both signals in a cell indicate newly formed neurons (Fig. 1).

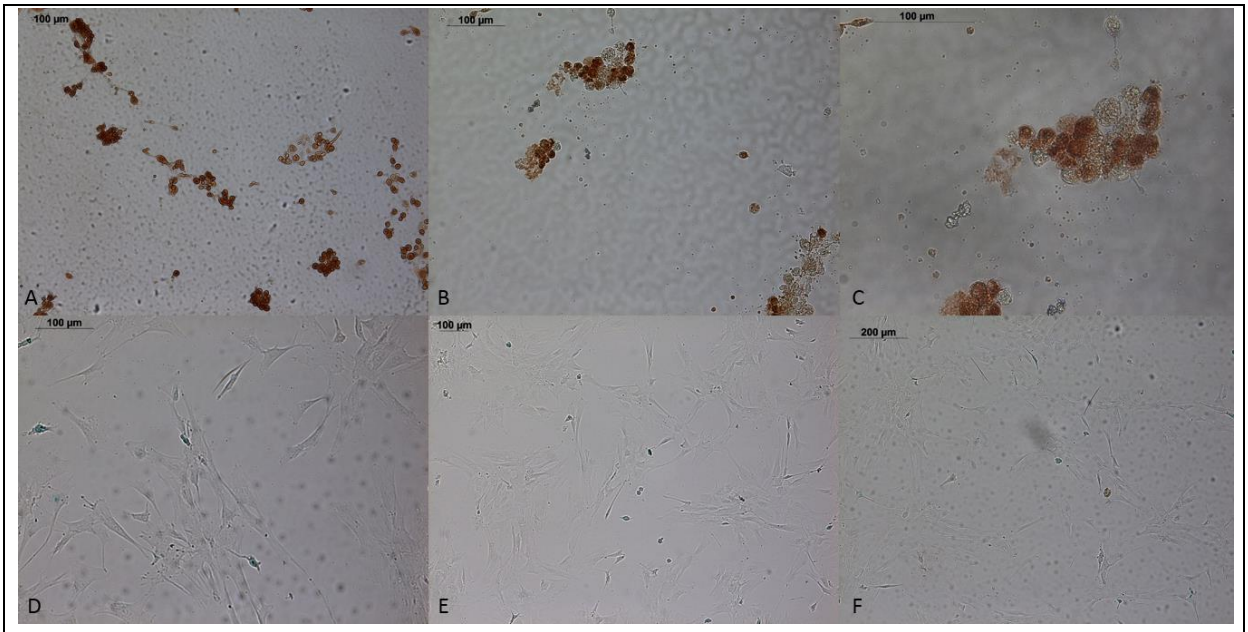

Figure 2: OE4-P2 cells, SAβG and PCNA-HRP immunocytochemistry results in bright field. Scale bar= 100 µm in figures (a), (b), (c), (d) and (e), in (f) scale bar =200 µm.

SaβG protocol stains the senescent cells in blue and PCNA expressing cells can be seen in brown as they are HRP conjugated. In tumor tissues, the cells proliferate uncontrollably, and the higher numbers of proliferating cells were expected. In Fig. 2 the cells with fibroblast-like shapes are stained for senescence whereas sphere-like cells are brown. The figure shows that the differentiated cells are senescent and non-differentiated cells are proliferating.

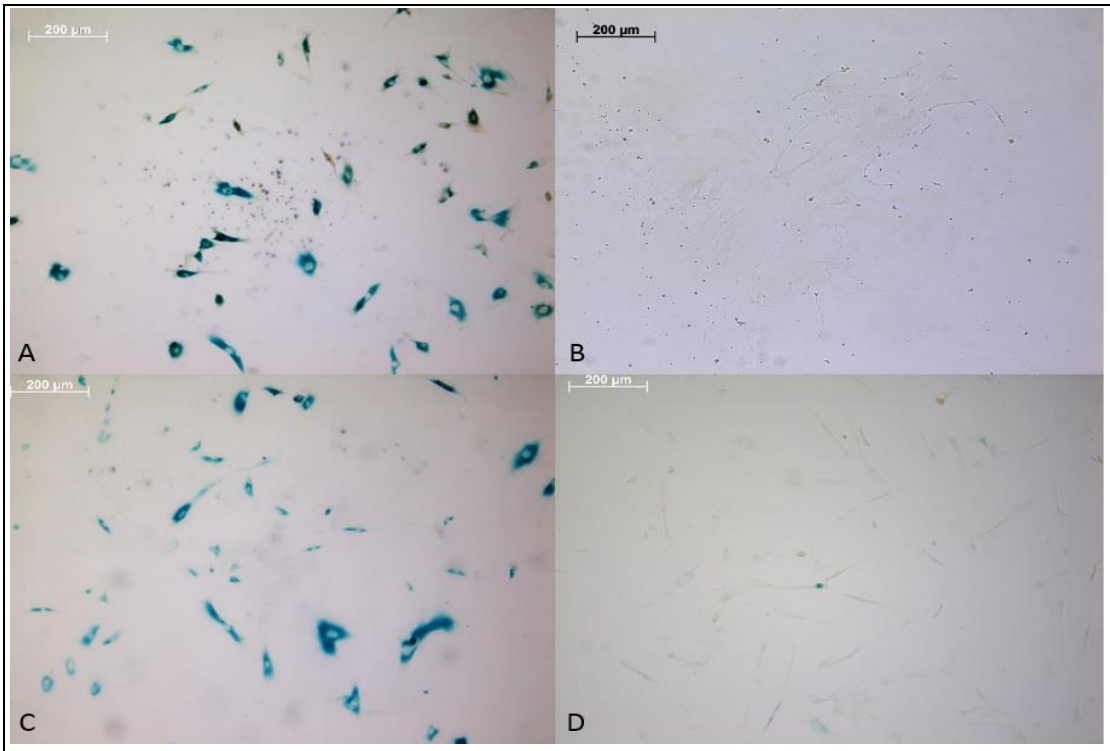

Figure 3: SAβG and immunostaining results. (a, b) OE6-P4 cells stained with BrdU-HRP and (c, d) OE7-P1 cells stained with PCNA-HRP, all scale bars = 200 µm.

A decrease in the total number of cells was observed after passage 4 (Fig. 3). Higher amounts of senescent cells were observed in OE6-P4 cells compared to OE7-P1 cells. The difference in overall cell numbers and senescent cell numbers could be due to the age difference or the differences between tumor types.

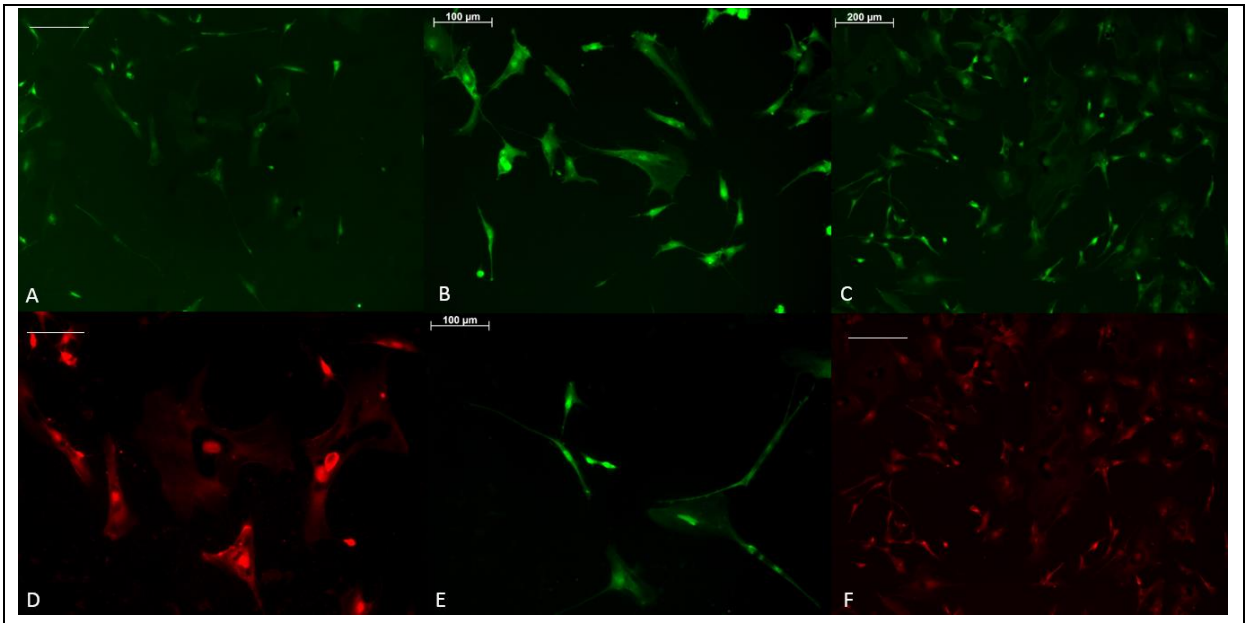

Figure 4: Immunostaining results of OE7-P1 cells. (a) PCNA staining, scale bar = 100 µm, (b) PCNA staining, scale bar= 100 mm, (c) PCNA staining, scale bar = 200 µm, (d) Sox2 staining, scale bar= 100 µm, (e) PCNA staining, scale bar=100 µm, (f) TAU staining of area in (c), scale bar= 200 µm.

OE7-P1 cells express proliferating cell characteristics as well as neural cell characteristics (Fig. 4). In Fig. 4 PCNA labeling (green) indicates proliferating cellsin Fig. 4d, neural stem cells expressing Sox2 are stained and Fig. 4f, TAU stained neurons can be seen. The presence of both TAU and PCNA signals in Fig. 4 c and f indicates the newly formed neurons.

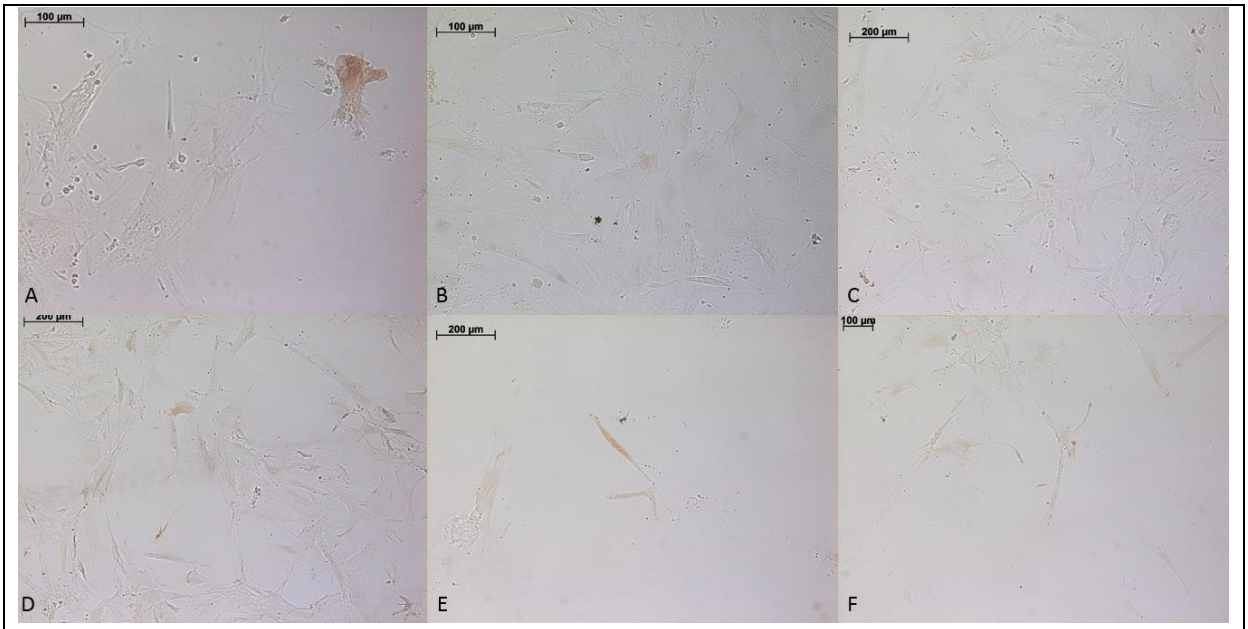

Figure 5: SAβG and BrdU-HRP immunostaining results of OE4-P5 cells. (a, b, f) scale bars = 100µm and (c,d,e) scale bars = 200 µm.

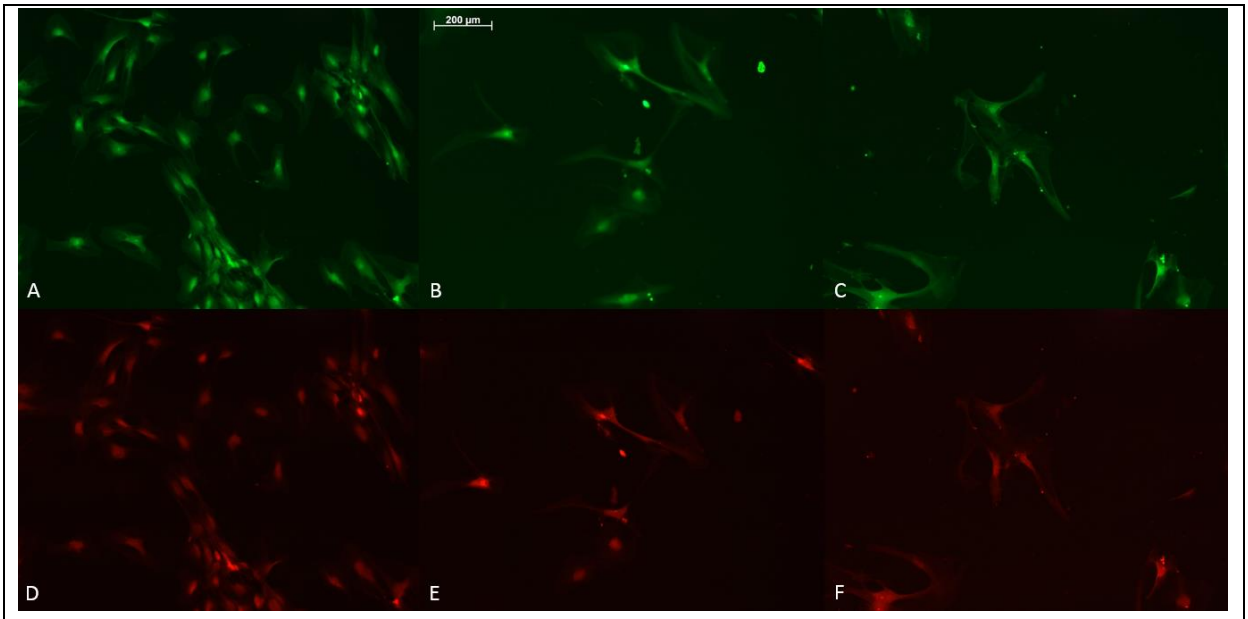

Figure 6: OE4-P5 immunocytochemistry results. (a) BrdU staining and (d) Sox2 staining of the same area. (b) BrdU staining, (e) Sox2 staining of the same area, (c) BrdU staining and (f) Sox2 staining of the same areas. Scale bar= 200µm.

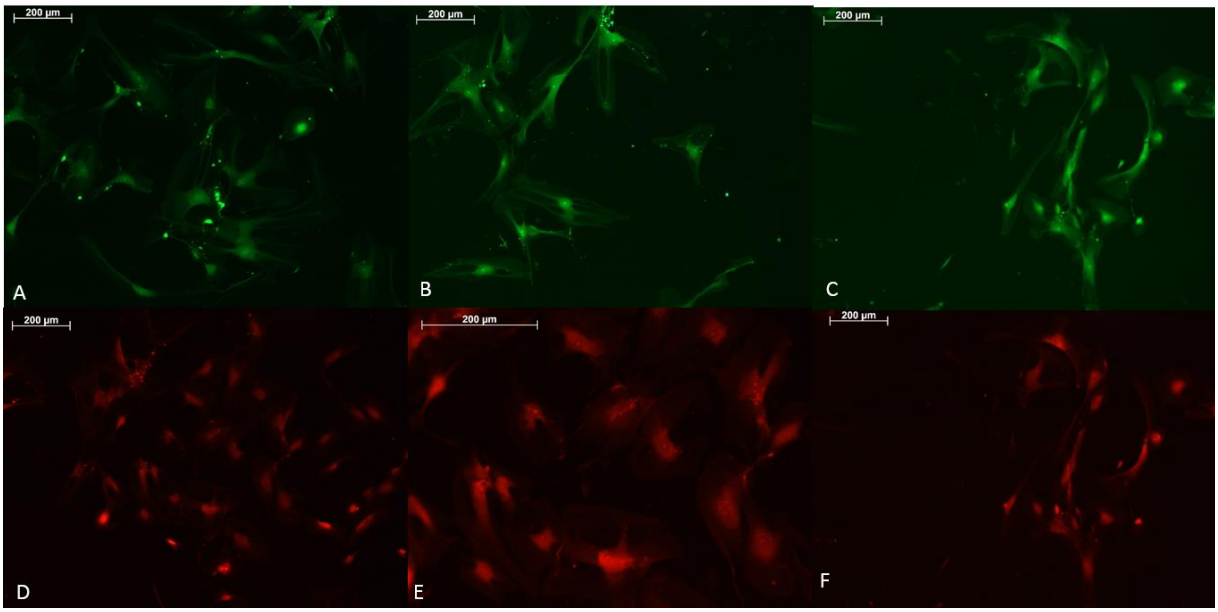

Figure 7: OE4-P5 immunostaining results. (a), (b) and (c) PCNA staining, and (e), (f), (g) Tau staining. (c) and (f) are the same area. Scale bar = 200µm.

OE4-P2 cells in Fig. 2 had a higher rate of proliferation than OE4-P5 cells in Fig. 5. SaβG staining for senescent cells is not as distinguishable as it is in Fig. 3 (OE6 and 7 cells). The reason could be the difference in tumor types. It can be speculated that the OE4 patient had a more aggressive sarcoma compared to OE6 and 7. In Fig. 5, BrdU-HRP staining can be seen,

suggesting that the cells are continuing to divide. Fig. 6 and 7 a, b, c also showed the cells were proliferating.

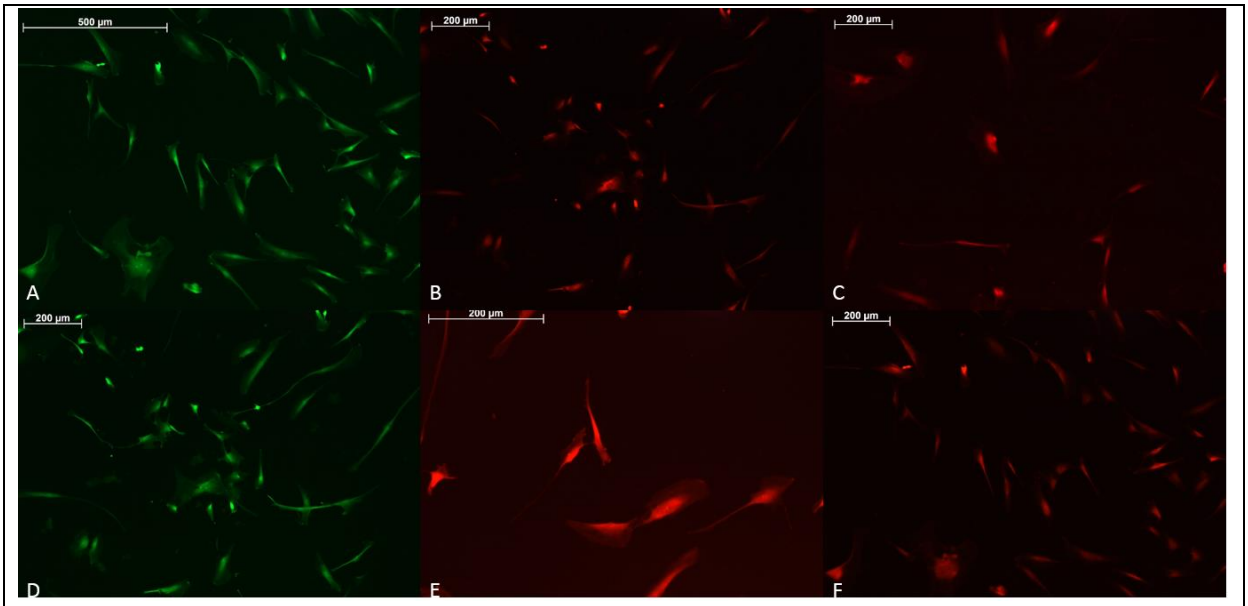

Figure 8: OE7-P1 immunostaining. (a) BrdU staining, scale bar = 500µm, (b) Sox2 staining, scale bar = 200 µm, (c) Sox2 staining, scale bar = 200 µm (d) PCNA staining, scale bar = 200 µm, (e) Tau staining scale bar = 500 µm, (f) Tau staining, scale bar = 200 µm.

OE7-P1 cells express proliferation markers in Fig. 8 a and d as well as neuron and stem cell markers, TAU in e and f and Sox2 in b and c, respectively.

In previous studies, it was found that BrdU, after 24 hours of exposure, decreases expressions of stem cell [42]. However, in Fig. 6 both BrdU and Sox2 positive cells can be seen, indicating that the BrdU was not effective enough to force the stem cells into senescence. This might be an indicator of cancer stem cell dominance in the cell culture. Comparison of Figures 1, 3 and 5 reveals that OE4 still has a higher proliferation rate after 5 passages, whereas OE7 cells have undergone senescence in the first passage. This could indicate that the stem cell reservoir of OE4 is larger than OE6 and 7, or has a higher proliferation rate. In both cases, this could be due to the metastatic nature of the OE4 tumor. It is known that metastatic cells have a higher proliferation rate than benign tumor cells, which may be the cause of the difference between OE4 cells' higher proliferation and lower senescence rate, and OE6 and OE7 cells.

2.4 CONCLUSION

The results show that stem cells were isolated from tumor tissues successfully and the stem cell numbers decreased with each passage. The cell culture obtained consisted of both mature neural cells and neural stem cells. The distinction of cancer and healthy stem cells could not be made based on the markers used in this study because both cancer stem cells and healthy stem cells are capable of self-renewal and proliferation, expressing Sox2. In order to maintain a population dominated by stem cells, EGF and FGF supplements could have been used which would keep the differentiation of stem cells at a minimum and increase the stem cell proliferation.

The original tumor cases should be investigated further for the stem cell properties of each to be understood. For the identification of differences in cancer stem cells caused by age, the variables should be kept to a minimum. The project was not carried out further due to the lack of funding. However, future studies aimed at examining the changes in telomere length are planned in order to identify the link between telomere length and cancer stem cell markers. By investigating the changes in the cancer stem cell markers' expression levels and find its relationship with telomere length in pathological tissues, a novel indicator for diagnostic use based on marker-telomere length associations could be found.

CHAPTER 3

Stem Cell Isolation from Old and Young Zebrafish Brains and RNA Expression Analysis

3.1 INTRODUCTION

Zebrafish is an ideal model organism to study human disease states, especially those regarding aging deficiencies. Zebrafish live up to 3 years in average and like humans, they age gradually [43–45]. Their genome is similar to human genome; for many human genes, a zebrafish ortholog has been identified [46]. Cognitive decline is observed with aging and it is under the influence of genetic and environmental factors [47]. Zebrafish have a brain that is comparable to a human's; forebrain, midbrain (consisting of the cerebellum, telencephalon, diencephalon) and hindbrain parts are established. They have an integrated nervous system and exhibit higher level processes such as memory and social behavior [45]. Neurogenesis in the human hippocampus, which is responsible for memory and learning has a comparable structure in the zebrafish brain which is the lateral pallium region [48].

Biological aging of the cells trigger the activation of cyclin-dependent kinase inhibitors (CDKI) and cause a cell cycle arrest. Senescent cells are stopped at the G1 phase of the cell cycle and do not go through S phase. For the cells to move to S phase, in order to replicate their DNA, E2F factors should be released from their inhibitory partner retinoblastoma protein (pRb). The release of E2F factors requires the phosphorylation of pRb by cyclin-dependent kinases (CDKs), especially CDK4/6 and CDK2. CDKIs have an active role in cellular aging and control the CDK's regulation. $P16^{INK4a}$ and $p15^{INK4b}$ inhibit CDK4/CDK6 and CDK2 is inhibited by $p21^{cip1}$ [49].

Arslan-Ergul et.al. have conducted a microarray analysis of samples from varying ages of zebrafish. In the two-group study; young (7.5 and 8.5 months old) and old (31 and 36 months old); the brains were removed as a whole and whole RNA isolation was performed. Following RNA isolation, microarray experiments were conducted in the attempt to find out differentially expressed elements between young and old zebrafish brain and validate the role of these elements during aging among individual animals. Next, gene ontology analysis was carried out to determine whether the differentially expressed genes were making a meaningful group. Old and young, and female and male ontology comparisons among genes that had significant expression differences were taken into consideration. Genes involved in brain development, angiogenesis, neurogenesis, cell differentiation and other processes were found to be significantly differentially expressed between groups. It was found that gene groups implicated in neurogenesis differed in expression levels, significantly, between young and old brains. Furthermore, the same gene group was differentially expressed between male and female fish; and the gene enrichment was in favor of young group (in the young-old comparison) and male group (in male-female comparison). Even among the genes functioning in bigger cellular processes (containing more than 9000 genes involved), the results were in favor of old and male groups [50].

In order to visualize neurogenesis in the fish brain, a BrdU staining procedure for zebrafish brain tissue sections has shown that the number of newly born neurons in the old zebrafish brain was lower than young zebrafish. The decrease in neurogenesis was more evident in the diencephalic ventricular zone within the telencephalon [51]. A recent study has shown that throughout aging, neurogenesis decreases significantly in zebrafish. A comparison between 3-months old and 6 months old zebrafish indicated a dramatic decrease in the formation of new neurons in the 6 months old group. Still, neurogenesis was demonstrated to be present in even 20-months old fish [52].

In the adult zebrafish brain, radial glial cells are capable of self-renewal, proliferation and producing neurons. There are two types of radial glial cells; type one cells are BrdU-, PCNA-, GFAP+, S100β+ and BLBP+, and type two cells that are BrdU+, PCNA+, GFAP+, S100β+, and BLBP+. Type one radial glial cells are in a quiescent state, they do not proliferate. Type two radial glial cells proliferate and differentiate to type 3 cells (neuroblast). Newborn neurons mostly settle in the subventricular zone during the development of the central nervous system. However, when neurogenesis is induced by brain damage, the newborn cells can migrate long distances to repair the damaged tissue [53]. The pathway that signals the cells to migrate is still unknown. Although it is known that the activation of stem cells decrease throughout aging, it is unknown which stem cell types decrease. It is believed that aging affects different stem cell types in different ways and neurogenesis continues in the regions that are related to certain brain functions [54]. In a more recent study, stem cells were isolated from the zebrafish brainstem. It was observed that the stem cells obtained were mitotically active but neuronal differentiation required the cells to escape cell cycle. This method enables the investigation of stem cells' interactions and different stem cell types of the zebrafish [55].

Within the scope of the project "Stem Cell Isolation from the Aging Zebrafish Brain",the main goal was to isolate and characterize the stem cells of zebrafish brain, and compare the young and old zebrafish neural stem cells' in terms of expressed markers. Neural stem cell culture was used to answer the following questions: 1) Do stem cells enter senescent state? 2) Do stem cells' phenotypic and metabolic properties change throughout aging? 3) Do the stem cell reserves in the brain decrease with age? The secondary goal was to identify the changes in gene expression in neural stem cells. Gene expression analysis from whole transcriptome sequencing was performed in order to find out how stem cells are affected by the global gene expressions, and which gene groups' activities increase or decrease through aging.

3.2 METHODS

3.2.1 Dissection and Stem Cell isolation

The fish were separated into two groups: young and old. The young fish were between 7-8 months old and the old fish were 25-28 months old. For total RNA extraction protocol, each group consisted of 5 fish, both wild-type AB strain. For immunocytochemistry protocol, the old group contained 3 fish, while the young group contained 9. The fish were anesthetized in ice cold water then decapitated. The animal protocol for this study was approved by the Local Animal Ethics Committee of Bilkent University (HADYEK) (see Appendix B for the copy of the ethics permission).

The heads of the fish were washed with 70% EtOH, the brains were put in ice cold L15 medium (21083-027, Gibco) containing 1% Penicillin-Streptomycin (15140-122, Gibco). Macs neural tissue dissociation kit (130-093-231, Miltenyi Biotec) was used for the isolation of neural stem cells. The solutions and enzymes were used according to the manual. The brain tissues were submerged into the solutions for 25 minutes at 28 ^{o}C with continuous rotation, then the brain tissue was cut into smaller pieces with the help of a fire polished pipette by pipetting up and down 20 times. Then the tissue pieces were pipetted with a smaller glass Pasteur pipette for 20 more times. The cell suspension was then put through a 70 µm cell strainer on a 15 ml falcon tube. The strainer was then rinsed with L15 containing 1% Pen-Strep and 5% FBS (washing medium) to collect the remaining cells. Then the solution was centrifuged at 1300 rpm for 10 minutes. The supernatant was discarded and the pellet was resuspended in washing medium and centrifuged at 1200 RPM for 8 minutes. The pellet was resuspended in 15 ml L15 containing 150 µl Pen-Strep, 750µl FBS, 3 µl 0.1 mg/ml Epidermal Growth Factor (PHG0314, Gibco) and 3 µl 0.1 mg/ml Fibroblast growth factor (PHG0024, Gibco). The cells were plated

in Laminin and Poly-D-Lysine coated slides for immunocytochemistry and for total RNA isolation experiments the cells were plated in bio-coated CellBind flasks (3290, Corning). The plates were kept in a non-CO_2 incubator at 28 ^oC. All of the cell culture medium was replaced the day after the cells were plated, half of the medium was changed on the second day [51].

3.2.2 Slide Coating

10 µg/ml poly-D-lysine (P7280-5mg, Sigma) was prepared and added directly to the slides and left in cell culture hood overnight at room temperature. Then the solution was removed and the slides were washed with water 3 times. The slides were air-dried and once completely dry, they were coated with 5 µg/ml laminin(23017-015, Gibco) in DMEM:F12 (11330-032, Gibco).

3.2.3 BrdU Treatment

Young fish were transferred from their tanks in the fish facility and placed in system water containing 30 µg/ml BrdU for 4 hours. Then anesthetized in ice-cold water and decapitated immediately after. Old fish were put into a separate tank with system water and ice cubes to keep the temperature around 12 ^oC. The fish were anesthetized and injected with 15 µl of 10 mg/ml BrdU intraperitoneally. After the injection, the fish were placed into another tank with system water at 28 ^oC and sacrificed after 4 hours. The young and old fish were treated differently due to the difference in their sizes and the difficulty in handling young fish and performing intraperitoneal injection. Stem cell isolation protocol was carried out following the decapitation of the fish.

3.2.4 Immunocytochemistry

First, the cells were washed with PBS twice, then they were fixed in ice-cold methanol for 10 minutes. The methanol was washed away with PBS, then 2 N HCl was added to the wells

dropwise and kept at 37 ^{o}C for 30 minutes, to permeabilize the cells. HCl was aspirated and the cells were washed with borate buffer (1.9 g Borax in 50 ml PBS) to inactivate HCl. This step was followed by PBS wash. The cells were blocked in goat serum (Sigma) for 30 minutes at room temperature, then were incubated with primary antibody at room temperature for an hour. Anti-NeuN (ab177487, Abcam), neuronal marker, anti-Sox2 (ab97959, Abcam), neural stem cell marker, anti-PCNA (ab29, Abcam), proliferation marker, anti-vimentin (ab8978), intermediate filament marker in radial glial cells, anti-Islet 1 (ab209977, Abcam), neural stem cell marker and anti-BrdU (5292S, Cell Signalling Technologies), proliferation marker, were the primary antibodies used. The antibodies were diluted in blocking buffer according to the Table 12. The cells were washed with 0.5% PBS-T 5 times in half an hour on shaker. Secondary antibody incubation was for 50 minutes at room temperature, Alexa 555 and 488 were used and diluted to 1:1000 in PBS-T. The cells were washed with PBS-T 5 times in half an hour. The coverslips were mounted on slides with ProLong Gold Antifade (P36930, Life Technologies).

Antibody	dilutions
anti-Neun	1/250
anti-PCNA	1/500
anti-BrdU	1/500
anti-Vimentin	1/100
anti-Islet	1/50
Anti-Sox2	1/500

Table 12: Antibody dilutions used

3.2.5 Total RNA isolation from cultured neural stem cells

Three to five days after the stem cells were plated, the cells were detached from the flask using StemPro Accutase (A11105-01, Gibco). RNeasy Mini Kit (74104, Qiagen) was used for the isolation of total RNA, the instructions of the kit were followed. The protocol consisted of the

following steps: lysis of the cells and protein contaminant reduction with β-mercaptoethanol (β-ME), precipitation of genetic material with 70% ethanol, column purification of RNA (discarding the DNA), washing and RNA elution. Next, in order to purify the RNA samples from the contaminating DNA, DNase treatment was performed with Ambion Turbo DNA-free Kit (AM1907, Ambion). Isolated and DNase-treated RNA samples' concentrations were measured with NanoDrop™ 2000.

3.2.6 RNA-Seq Methods

RNA sequences isolated (by Begun Erbaba) were sent to TUBITAK MAM and were sequenced using Illumina HiSeq 2500 system. Sequence data received was analyzed for expression differences between samples.

3.2.6.1 System Specifications

CPU:Intel i5-3337U

GPU: NVIDIA GeForce GT740m

RAM: 8 GB

HDD/SSD: SeaGate 500GB 5400RPM

OS: Ubuntu 16.04

3.2.6.2 Preprocesses

For checking the quality of the RNA sequence data obtained from TUBITAK, FastQC analysis program was run. Fastqc does raw sequence data quality checks and provides information on whether the data is contaminated with adapter sequences or has any problems that should be considered and corrected before the next steps of RNA-sequence analysis.

The zebrafish (*Danio rerio*) genome, version GRCz10, was downloaded from Ensembl database [56]. The folder downloaded contained soft masked and repeat masked fasta files as well as non-masked files of each chromosome of zebrafish. Since "masked" reads mean that the repetitive parts of the reference genome are masked, the bases are converted to "N"s, thus if the RNA to be aligned to the reference genome cannot be aligned to the repeats resulting in a false mapping of the reads. Thus, the unmasked genome files were used. In order to minimize the time consumed by running Bowtie2 separately with each genome file, fasta files of each chromosome were concatenated. The concatenation process takes short time with popular Linux command: "cat". Fig. 9 shows the color coding in sample command lines from Fig. 9 to 16, and the sample command line used for the "cat" function.

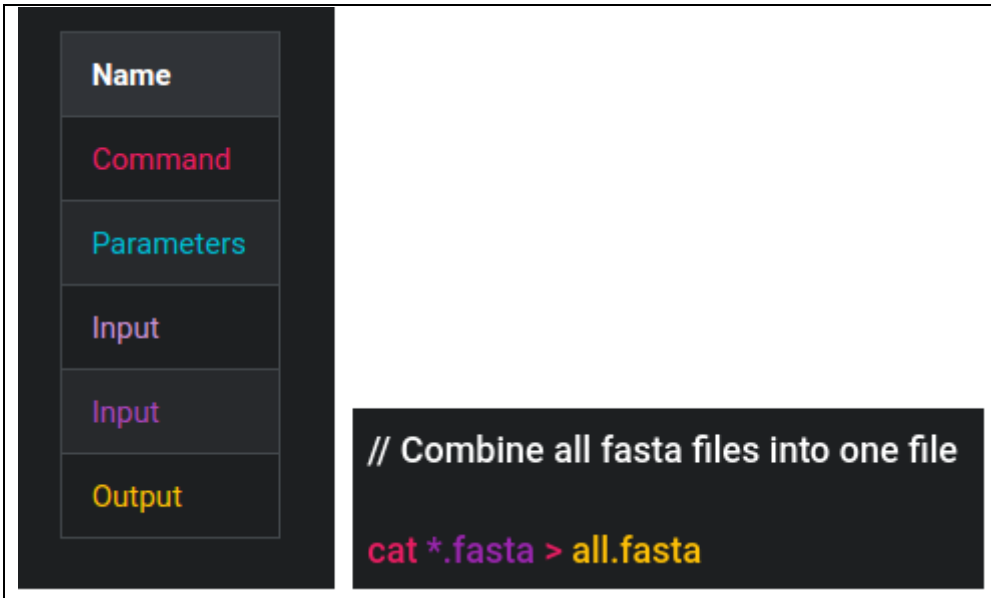

Figure 9: Color coding of the sample command lines and concatenation of genome containing .fasta files into one .fasta file

3.2.6.3 RNA-Seq Analysis

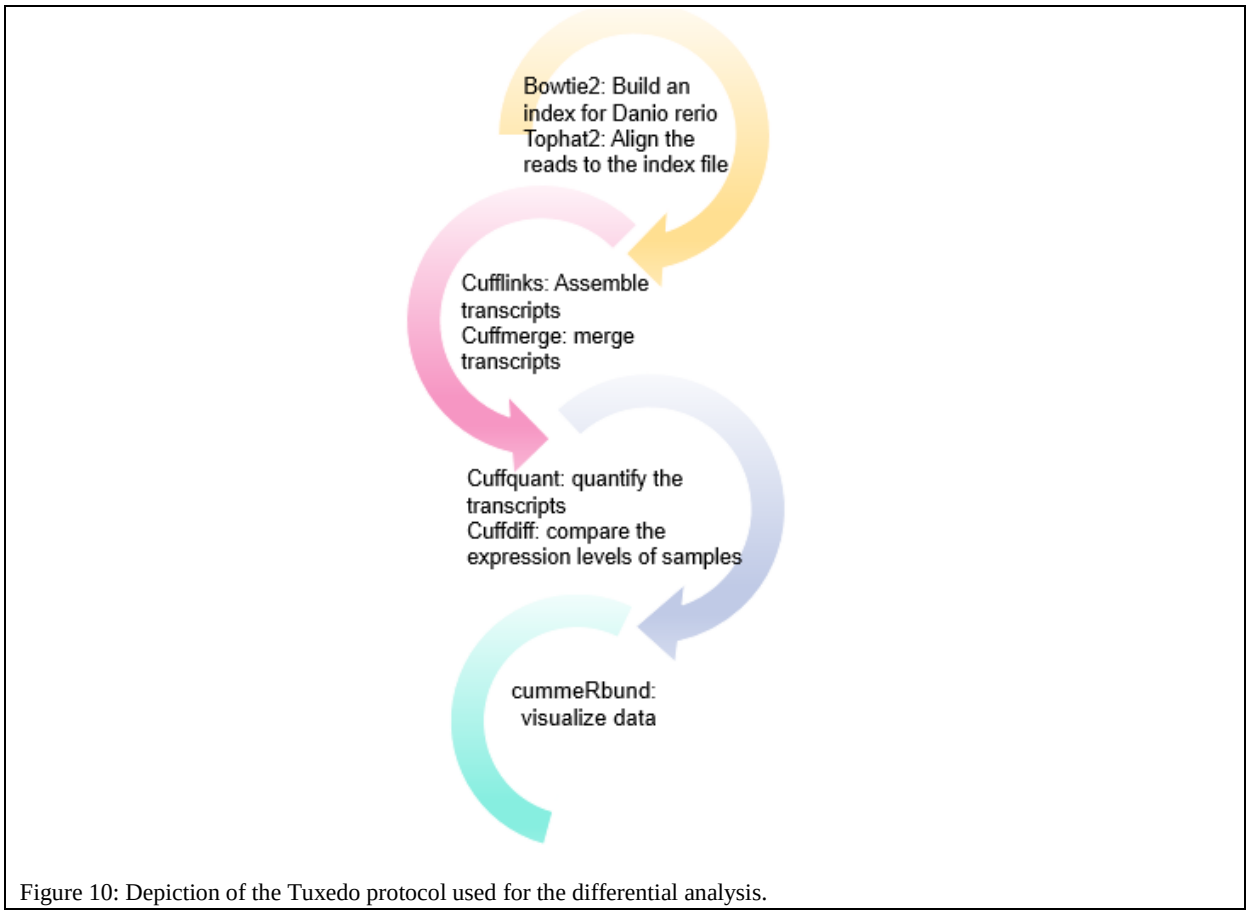

Figure 10: Depiction of the Tuxedo protocol used for the differential analysis.

The pipeline used in this study is depicted in Fig. 10. Bowtie2, which is the first step of the pipeline, is a fast, short read aligner that maps the FASTQ reads to a reference sequence. Transcriptome or reference genome could be used for aligning the reads. However, transcriptome alignment may exclude transcripts that are not annotated. Thus, I mapped the reads to the reference genome and used the "build" command of BowTie2 to create an index from the genome file obtained from the Ensembl database. Since our reads vary in length, a short read mapper was not preferred, TopHat was used instead for the alignment. Bowtie2 takes the concatenated fasta file that contained the reference genome of zebrafish as an argument and it builds the index folder containing .bt2 files.

```
// Build an index of the reference genome

bowtie2-build --threads 8 /fasta/all.fa /index/danio_rerio
```

Figure 11: Command line sample for bowtie2 tool

TopHat2 was used to align reads from each group (old and young) to the reference genome. It is used for aligning reads to the reference genome. Transcripts contain introns and may span exon-exon junctions. Hence the tool for aligning the RNA-Seq reads must be capable of identifying exon-exon junctions by splitting reads. TopHat2 utilizes Bowtie2 which identifies split reads by looking for "coverage islands". Coverage islands are regions with read coverage, the tool looks for continuous regions or closely related regions with coverage that are separated by non-coverage regions that correspond to introns or untranscribed regions and tries to find if the coverage regions are transcripts of the same gene.

```
// Align the reads to the reference index

tophat2 /index/danio_rerio RNAold_GTGAAA_R1.fastq.gz RNAold_GTGAAA_R2.fastq.gz
```

Figure 12: Command line sample for tophat2 tool

For alignment, TopHat2 takes the output of Bowtie2, the index file, and the reads as inputs (Fig. 12) and gives .bam files as output. The output files contain mapped and unmapped reads as well as deletions and insertions. The alignment process with TopHat2 takes longer to align reads to the reference genome than Bowtie2 takes for building an index.

Next, Cufflinks was used. Cufflinks assembles transcripts and estimates fragments per kilobase million (FPKM). A gene may contain more than one transcript that are of multiple exons. Multiple transcripts of the gene share exons, thus the reads align probabilistically (different isoforms of a gene have different expression values). FPKM is a unit of measurement where

the counts are normalized for sequencing depth and gene length. First, the total count of a sample is divided by a million, for the “per million” scaling. Then the read count of a certain gene is divided by the scaling factor obtained in the previous step, this gives the “fragments per million” (FPM) value. Finally, the FPM value is divided by the length of the gene, in kilobases, resulting of the normalized data of FPKM. Cufflinks was given aligned old or young RNA-seq files obtained from TopHat2 and annotation file downloaded from Ensembl database (.gtf file), and it output 2 .gtf files, and 2 fpkm files.

```
// Assemble transcripts and estimate FPKM

cufflinks -o cufflinks_output/young -G ../Zebrafish/gtf/Danio_rerio.GRCz10.85.gtf -p 8 -b ../fasta/all.fa -u tophat_young_out/accepted_hits.bam
```

Figure 13: Command line sample for cufflinks tool.

When dealing with multiple RNA-seq samples, combining the data into a set of transcripts is a helpful step before performing comparative analysis. Replicates of each condition (young and old) are aligned to the reference transcriptome annotation (.gtf file) and merges all of the samples assemblies. This way Cuffmerge rescues less expressed genes that may not have full reconstruction in each replicate. Cuffmerge takes transcripts.gtf files obtained from Cufflinks for each sample, annotation .gtf file from ensemble database and reference genome .fasta file and returns a merged.gtf file.

```
// Merge transcripts

cuffmerge -p 8 -g ../Zebrafish/gtf/Danio_rerio.GRCz10.85.gtf -s ../fasta/all.fa -o merged_assembly assembly_GTF_list.txt
```

Figure 14: command line sample for cuffmerge tool, the use of this tool is optional.

Cuffquant provides quantification of gene expression levels. The output of TopHat (.bam file) and merged.gtf file obtained from cuffmerge is fed into cuffquant, the output (.cxb) file is used in the following step cuffdiff for further processing.

```
// Quantify the gene expressions

cuffquant -p 8 -o cuffquant_young_output merged_assembly/merged.gtf tophat_young_out/accepted_hits.bam
```

Figure 15: command line sample for Cuffquant tool.

Cuffdiff is the tool that compares the expression levels of genes from different samples. Merged.gtf file and cuffquant output files for each sample is given to cuffdiff as an input and the results are output in FPKM tracking files.

```
// Compare the gene expressions

cuffdiff -p 8 -o cuffdiff_output -L old,young -u merged_assembly/merged.gtf cuffquant_old_output/abundances.cxb cuffquant_young_output/abundances.cxb
```

Figure 16: command line sample for cuffdiff tool.

The final step of the differential expression analysis is the visualization of the data. CummeRbund was used to analyze the results of RNA-Seq data from the output of cuffdiff. CummeRbund stores data from the output files of cuffdiff analysis in a local SQLite database in order to speed up access to certain features contained such as isoforms, genes CDS. The data elements can be manipulated through RSQLite package enabling fast access and search in upcoming analyses [57].

3.3 RESULTS and DISCUSSION

3.3.1 RNA-Seq Analysis

	gene_id	gene	locus	sample_1	sample_2	status	value_1	value_2	log2(fold_	test_stat	p_value	q_value	significan
2	XLOC_000074	si:ch211-160d14.9	1:7903118-7905898	old	young	OK	208.161	0	#NAME?	#NAME?	5,00E-05	0.025082	yes
3	XLOC_000171	U3	1:15765587-15765803	old	young	OK	9631.43	3129.16	-162.198	-545.369	5,00E-05	0.025082	yes
4	XLOC_000243	fabp2	1:25157401-25160746	old	young	OK	595.753	138.337	-210.653	-519.505	0.0001	0.043893	yes
5	XLOC_000630	si:ch211-114l13.11	1:57191806-57195910	old	young	OK	0	277.186	inf	#NAME?	5,00E-05	0.025082	yes
6	XLOC_000883	ugt8	1:19863129-19914215	old	young	OK	61.078	252.883	-127.218	-423.463	5,00E-05	0.025082	yes
7	XLOC_002538	Metazoa_SRP	11:11445771-11446068	old	young	OK	287.643	0	#NAME?	#NAME?	5,00E-05	0.025082	yes
8	XLOC_002542	Metazoa_SRP	11:11477184-11477481	old	young	OK	898.886	0	#NAME?	#NAME?	5,00E-05	0.025082	yes
9	XLOC_002582	Metazoa_SRP	11:12636307-12636604	old	young	OK	898.886	0	#NAME?	#NAME?	5,00E-05	0.025082	yes
10	XLOC_002583	Metazoa_SRP	11:12654040-12654337	old	young	OK	431.465	485.353	-315.214	-66.991	5,00E-05	0.025082	yes
11	XLOC_003082	Metazoa_SRP	11:11400211-11400509	old	young	OK	483.445	233.503	-437.184	-765.714	5,00E-05	0.025082	yes
12	XLOC_003110	Metazoa_SRP	11:12185739-12186033	old	young	OK	163.807	0	#NAME?	#NAME?	5,00E-05	0.025082	yes
13	XLOC_007129	fam101b	15:25160766-25164414	old	young	OK	160.899	347.602	-221.065	-481.627	5,00E-05	0.025082	yes
14	XLOC_007234	mag	15:34033828-34075811	old	young	OK	102.186	318.285	-168.281	-437.663	5,00E-05	0.025082	yes
15	XLOC_007342	si:ch211-181d7.3	15:42785206-42804045	old	young	OK	104.108	281.362	143.435	441.515	5,00E-05	0.025082	yes
16	XLOC_008222	tuft1a	16:22448309-22470315	old	young	OK	454.095	19.538	-121.671	-383.111	0.0001	0.043893	yes
17	XLOC_009134	actc1b	17:117123-124703	old	young	OK	0	225.304	inf	#NAME?	5,00E-05	0.025082	yes
18	XLOC_011707	cx47.1	2:3641652-3667272	old	young	OK	276.602	76.947	-184.587	-468.858	5,00E-05	0.025082	yes
19	XLOC_012221	crlf1a	2:42027176-42071214	old	young	OK	147.435	476.921	-162.826	-526.367	5,00E-05	0.025082	yes
20	XLOC_014617	C7 (1 of many)	21:20706239-20896022	old	young	OK	120.898	184.179	-271.461	-830.283	5,00E-05	0.025082	yes
21	XLOC_015225	tlcd1	21:26043519-26053269	old	young	OK	403.111	911.963	-214.413	-482.731	5,00E-05	0.025082	yes
22	XLOC_020689	cldnk	3:49088238-49092400	old	young	OK	271.625	630.991	-210.592	-496.927	5,00E-05	0.025082	yes
23	XLOC_020706	aatka	3:51644914-51657356	old	young	OK	141.172	531.817	-140.845	-397.503	5,00E-05	0.025082	yes
24	XLOC_021616	si:dkey-51d8.9	4:44380152-44388931	old	young	OK	0	289.684	inf	#NAME?	5,00E-05	0.025082	yes
25	XLOC_022170	znf1017	4:69735177-69740287	old	young	OK	247.999	0	#NAME?	#NAME?	5,00E-05	0.025082	yes
26	XLOC_022246	ms4a17a.10	4:75168276-75208498	old	young	OK	0	281.164	inf	#NAME?	5,00E-05	0.025082	yes
27	XLOC_023961	si:dkey-27p18.3	5:21902871-21920696	old	young	OK	318.278	0	#NAME?	#NAME?	5,00E-05	0.025082	yes
28	XLOC_024048	vamp5	5:27697096-27707317	old	young	OK	157.025	530.939	-156.438	-487.454	5,00E-05	0.025082	yes
29	XLOC_027085	cd82a	7:26438057-26466929	old	young	OK	220.888	998.422	-114.559	-385.382	0.0001	0.043893	yes
30	XLOC_027602	HIST2H3A (1 of many)	7:6208862-6209690	old	young	OK	0	328.826	inf	#NAME?	0.0001	0.043893	yes
31	XLOC_027836	serpine1	7:25994390-25998821	old	young	OK	182.376	450.415	130.434	44.073	5,00E-05	0.025082	yes
32	XLOC_028160	ENSDARG00000079660	7:64323603-64350388	old	young	OK	105.975	0	#NAME?	#NAME?	5,00E-05	0.025082	yes
33	XLOC_031040	ENSDARG00000099056	KN150683.1:2653-9949	old	young	OK	293.701	0	#NAME?	#NAME?	5,00E-05	0.025082	yes
34	XLOC_000001	cep97	1:6407-16373	old	young	OK	72.605	560.029	-0.374567	-0.145399	0.7891	0.997011	no
35	XLOC_000002	nfkbiz	1:18715-23389	old	young	NOTEST	0.541484	115.137	108.837	0	1	1	no

Table 13: gene_exp.diff file obtained from cuffdiff output folder listing the comparison of genes between sample groups, young and old, expression values in FPKM and significance levels (yes or no).

Cuffdiff compared 31077 genes between samples and found that the expression levels of 34 genes are significantly different between samples (Table 13). However, some of the expression values were 0 which indicates the absence of data and a numerical significance cannot be assigned to the statistical significance of the expression comparison. Hence the genes with 0 FPKM values in either sample were omitted (Table 14).

	gene_id	gene	locus	sample_1	sample_2	status	value_1	value_2	log2(fold_	test_stat	p_value	q_value	significant
2	XLOC_000	fabp2	1:2515740	old	young	OK	595753	138337	-210653	-519505	0.0001	0.0438938	yes
3	XLOC_008	tuft1a	16:224483	old	young	OK	454095	19538	-121671	-383111	0.0001	0.0438938	yes
4	XLOC_027	cd82a	7:2643805	old	young	OK	220888	998422	-114559	-385382	0.0001	0.0438938	yes
5	XLOC_000	U3	1:1576558	old	young	OK	9631.43	3129.16	-162198	-545369	0,00005	0.0250821	yes
6	XLOC_000	ugt8	1:1986312	old	young	OK	61078	252883	-127218	-423463	0,00005	0.0250821	yes
7	XLOC_002	Metazoa_	11:126540	old	young	OK	431465	485353	-315214	-66991	0,00005	0.0250821	yes
8	XLOC_003	Metazoa_	11:114002	old	young	OK	483445	233503	-437184	-765714	0,00005	0.0250821	yes
9	XLOC_007	fam101b	15:251607	old	young	OK	160899	347602	-221065	-481627	0,00005	0.0250821	yes
10	XLOC_007	mag	15:340338	old	young	OK	102186	318285	-168281	-437663	0,00005	0.0250821	yes
11	XLOC_007	si:ch211-1	15:427852	old	young	OK	104108	281362	143435	441515	0,00005	0.0250821	yes
12	XLOC_011	cx47.1	2:3641652	old	young	OK	276602	76947	-184587	-468858	0,00005	0.0250821	yes
13	XLOC_012	crlf1a	2:4202717	old	young	OK	147435	476921	-162826	-526367	0,00005	0.0250821	yes
14	XLOC_014	C7 (1 of m	21:207062	old	young	OK	120898	184179	-271461	-830283	0,00005	0.0250821	yes
15	XLOC_015	tlcd1	21:260435	old	young	OK	403111	911963	-214413	-482731	0,00005	0.0250821	yes
16	XLOC_020	cldnk	3:4908823	old	young	OK	271625	630991	-210592	-496927	0,00005	0.0250821	yes
17	XLOC_020	aatka	3:5164491	old	young	OK	141172	531817	-140845	-397503	0,00005	0.0250821	yes
18	XLOC_024	vamp5	5:2769709	old	young	OK	157025	530939	-156438	-487454	0,00005	0.0250821	yes
19	XLOC_027	serpine1	7:2599439	old	young	OK	182376	450415	130434	44073	0,00005	0.0250821	yes

Table 14: gene_exp.diff file after the genes with 0 FPKM values were deleted from the list. Sorted according to q-values.

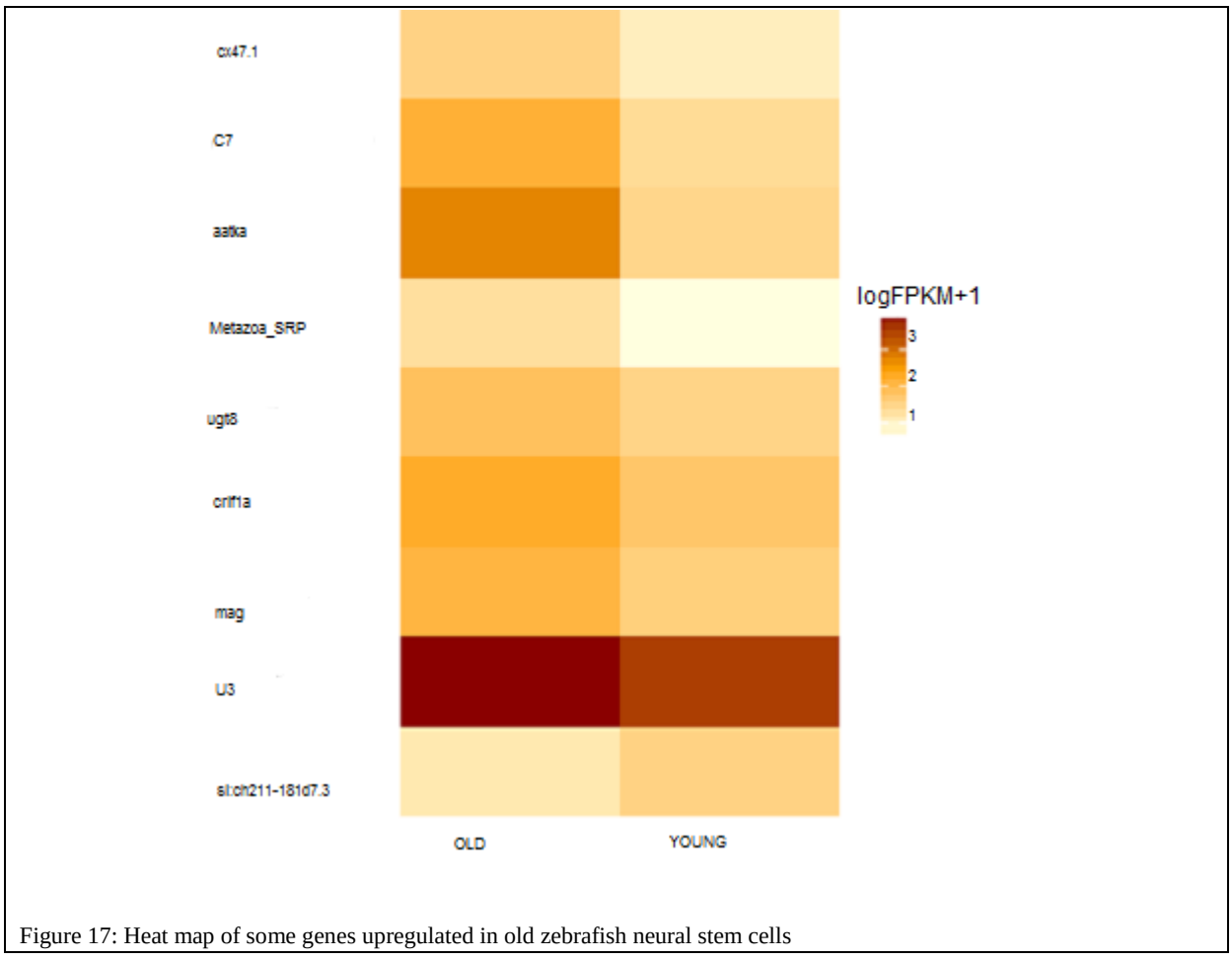

Figure 17: Heat map of some genes upregulated in old zebrafish neural stem cells

Fig. 17 shows the heat map generated with cummerbund, an R package. The first 9 genes that are differentially expressed are depicted in the figure. FABP2, Tuft1a, Cd82a, U3, fam101b,

Ugt8, Metazor_SRP, crlf1a, Mag, cx47.1, c7, Tlcd1, cldnk, Aatka and VAMP5 are the genes found to have a significantly higher expression level in old zebrafish neural stem cells compared to young zebrafish stem cells.

FABP2 is a member of FABPs (fatty acid binding proteins), which are thought to play a role in the intracellular transport of long-chain fatty acids and responsible in the modulation of cell growth and proliferation. FABP2 is implicated in triglyceride-rich lipoprotein synthesis. FABP2 has a human ortholog associated with insulin resistance in the FABP2 allele with threonine at codon 54 (instead of alanine) [58]. FABP2 is one of the genes highly expressed in old zebrafish neural stem cells compared to the young. This expression difference was expected as insulin resistance develops with age. Tuftelin (Tuft1a) is another gene upregulated in old zebrafish neural stem cells. It is an acidic protein that is thought to play a role in dental enamel mineralization and is implicated in caries susceptibility. It is also thought to be involved in mesenchymal stem cell function, and neurotrophin nerve growth factor mediated neuronal differentiation. It has a human ortholog, which is implicated in the most common genetic disease of the dental enamel, Amelogenesis Imperfecta, and expressed in ameloblastoma, an odontogenic tumor, that originate from the mandible (lower jaw) most commonly [59]. The loss of neurons in adult zebrafish brain is supported by the stem cell subpopulation in the brain. Thus, the stem cells may be differentiating into mature cells in old zebrafish more frequently than in young fish. Cd82a is a metastasis suppressor gene product, which is a membrane glycoprotein that is a member of the transmembrane 4 superfamily. Expression of this gene has been shown to be downregulated in tumor progression of human cancers and can be activated by p53 through a consensus binding sequence in the promoter. Cd82 was identified as a potential organizer in the regulation of cell proliferation and glial activation in case of CNS damage [60]. Cd82a increase in old zebrafish may also support the hypothesis of old zebrafish producing more mature central nervous system cells than young zebrafish. It was also found

that U3, a non-coding RNA, was expressed more highly in old zebrafish neural stem cells. The product of this gene is found predominantly in the nucleolus and is thought to guide site-specific cleavage of ribosomal RNA (rRNA) during pre-rRNA processing. U3 was reported to have high expression levels in breast cancer tissue [61]. The high expression of U3 in old fish might indicate age-related tumor formations in zebrafish.

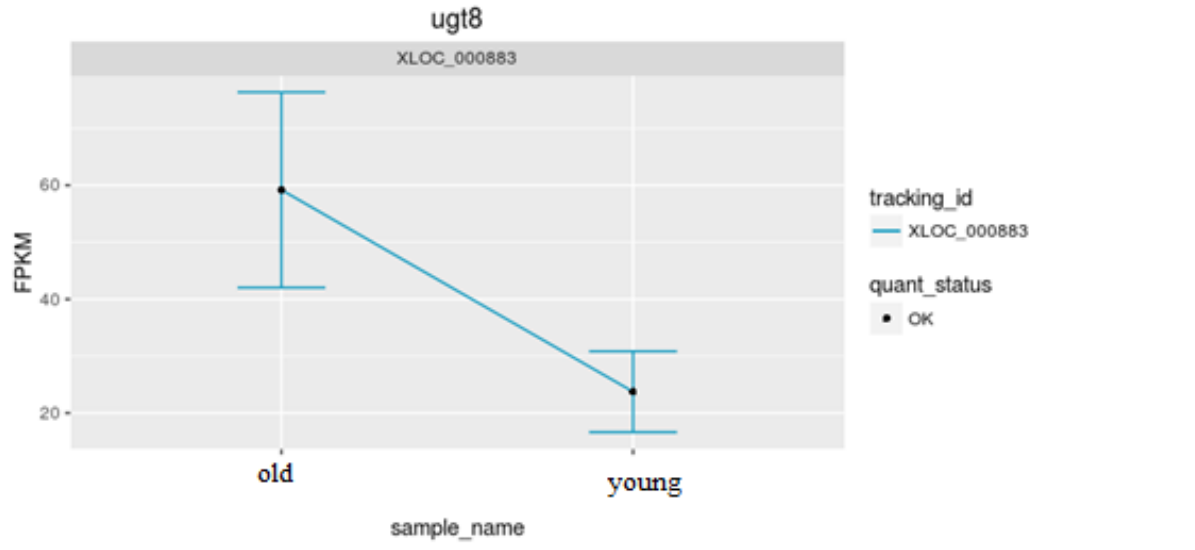

Figure 18: Ugt8 expression difference graph generated in R by cummeRbund package.

Ugt8 was downregulated in young zebrafish brain, as depicted in Fig. 18. Ugt8 is a member of UDP-glycosyltransferase family. It is involved in the sphingolipid production of the myelin membrane of central and peripheral nervous systems. UGT8 was found to be important in the differentiation of oligodendrocytes in humans [62]. As the expression differences of Tuft1a, cd82 and U3 indicate, Ugt8 also supports the hypothesis that old zebrafish stem cells are differentiating more often than they are proliferating.

Metazoa_SRP is a signal recognition particle RNA and is the RNA component of the signal recognition particle (SRP) ribonucleoprotein complex. SRP is a universally conserved ribonucleoprotein that directs the traffic of proteins within the cell and allows them to be secreted. The SRP RNA, together with one or more SRP proteins contribute to the binding and release of the signal peptide. The RNA and protein components of this complex are highly

conserved [56]. The expression difference of Metazoa_SRP should be investigated further as it may mean there is more signal trafficking in old zebrafish neural stem cells than young zebrafish.

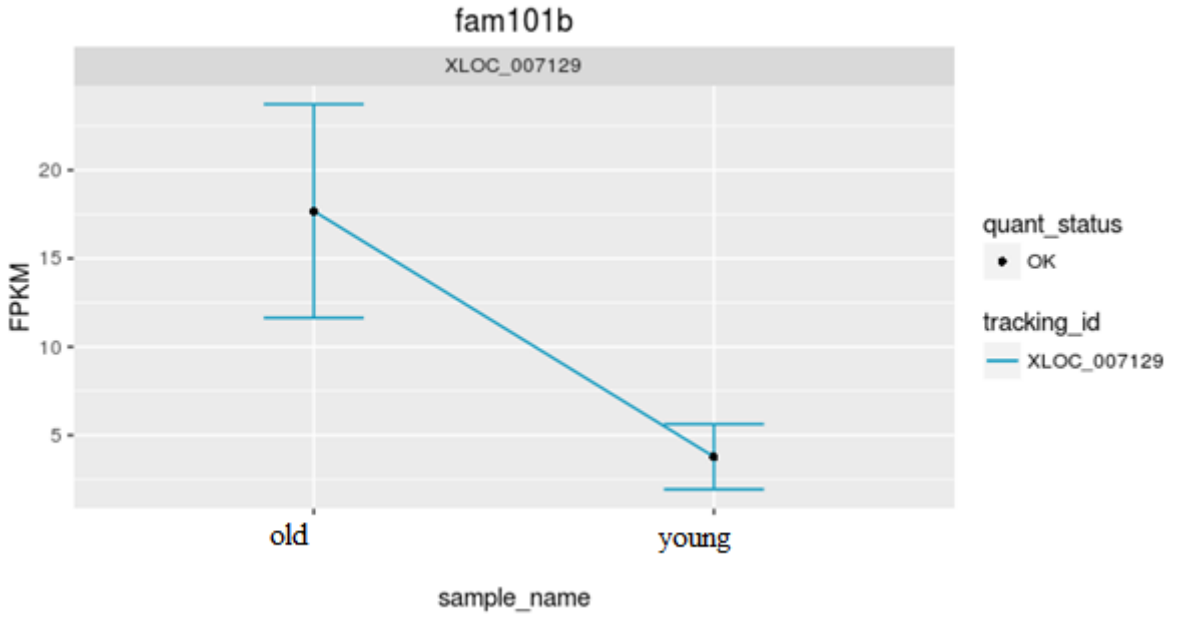

Figure 19: fam101b expression difference graph generated in R by cummeRbund package.

Fam101b is another differentially expressed gene, it is expressed in higher amounts in old fish neural stem cells compared to the young (Fig. 19). Fam101b is involved in the regulation of the perinuclear actin network and nuclear shape through interaction with filamins [56]. MAG protein is thought to be involved in the process of myelination. It is a lectin that binds to sialylated glycoconjugates and mediates certain myelin-neuron cell-cell interactions. The decreased expression of MAG was correlated with reduced neurofilament spacing and phosphorylation. It was found that the maturation and viability of myelinated axons were regulated by MAG protein [63].

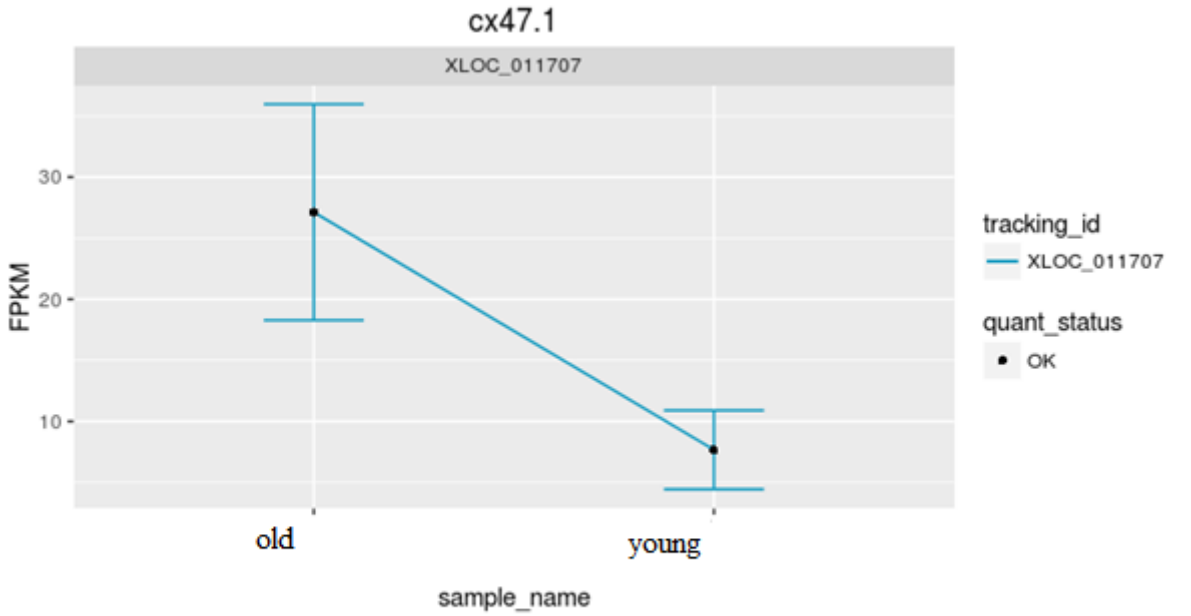

Figure 20: Cx47.1 expression difference graph generated in R by cummeRbund package.

Cx47.1, the human ortholog of this gene encodes a gap junction protein. One gap junction consists of a cluster of closely packed pairs of transmembrane channels, the connexins, through which materials of low MW diffuse from one cell to a neighboring cell. It may play a role in myelination in central and peripheral nervous systems [64]. It was found to be highly expressed in old zebrafish neural stem cells (Fig. 20).

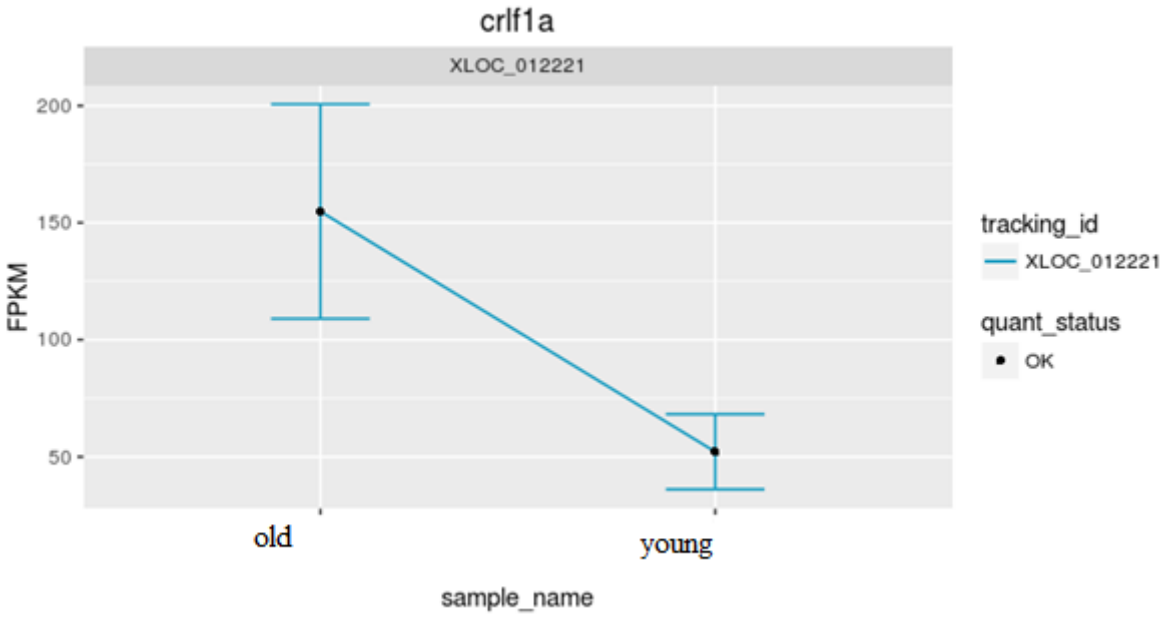

Figure 21: Crlf1a expression difference graph generated in R by cummeRbund package.

Crlf1a was downregulated in young fish brain stem cells (Fig. 21). Crlf1a gene encodes a member of the cytokine type I receptor family. The protein forms a secreted complex with cardiotrophin-like cytokine factor 1 and acts on cells expressing ciliary neurotrophic factor receptors. The complex can promote survival of neuronal cells. A mutation in the gene was reported to be causing Crisponi syndrome, an autosomal recessive disorder with low incidence levels [65]. It can be speculated that the old zebrafish stem cells are compensating for the decline of cognitive decline by promoting the survival of neurons.

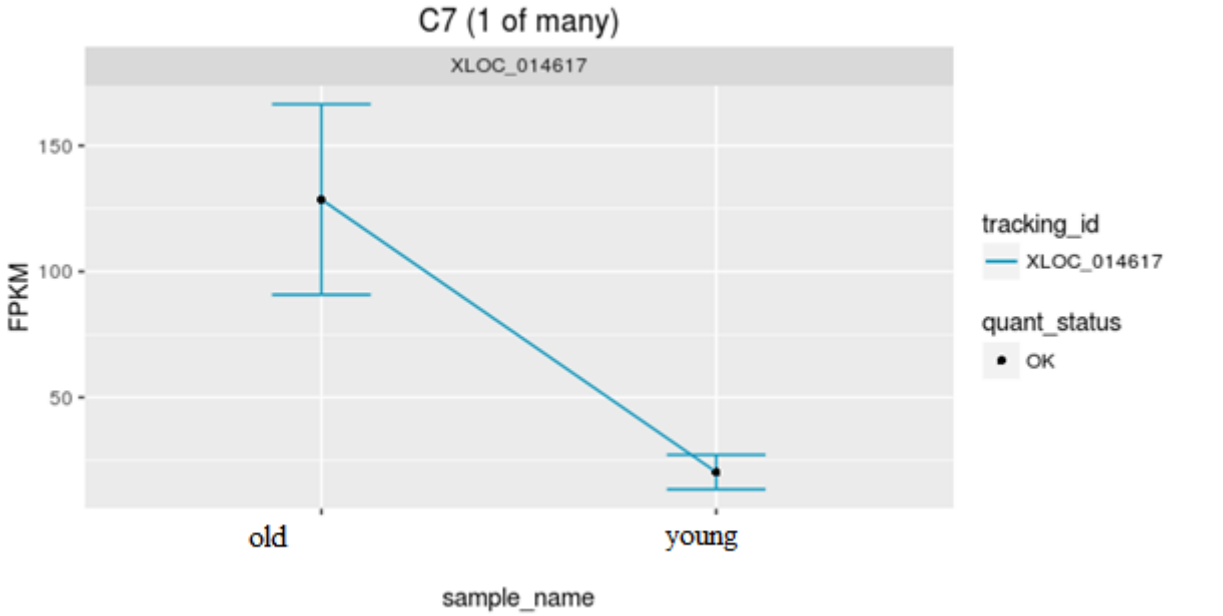

Figure 22: C7 expression difference graph generated in R by cummeRbund package.

C7 gene was found to be upregulated in old fish neural stem cells as demonstrated in Fig. 22. This gene encodes a serum glycoprotein that forms a membrane attack complex together with complement components C5b, C6, C8, and C9 as part of the terminal complement pathway of the innate immune system. This protein initiates membrane attack complex formation by binding the C5b-C6 subcomplex and inserts into the phospholipid bilayer, serving as a membrane anchor. Studies found a possible link between C7 downregulation and decrease in neutrophil chemotaxis and opsonization [66]. It was also reported that esophageal tumor cells do not express C7 [67]. This may be the indicator of age-related loss of neuronal cells.

Tlcd1 is a calcium channel facilitator that increases calcium flux by generating a larger window current and slowing inactivation of the L-type CACNA1C/CaV1.2 channel. It was found to be less expressed in young neural stem cells compared to the old. It is required for the neural plate formation [68]. This also supports the finding of increased Metazoa_SRP, as both point to an increase in the signaling traffic. Both imply that the old brain neural stem cells have busy intercellular communications. Cldnk gene encodes a member of the claudin family. Claudins

are integral membrane proteins and components of tight junction strands. Tight junction strands serve as a physical barrier to prevent solutes and water from passing freely through the paracellular space between epithelial or endothelial cell sheets. It is involved in myelin formation through CNS development to adult regeneration in zebrafish [69].

Aatka is induced during apoptosis, and expression of this gene may be a necessity for the induction of growth arrest and/or apoptosis of myeloid precursor cells. The increase in the expression of this gene in old zebrafish may be an indicator of the increase in age-related tumor formation. This gene has been shown to induce neuronal differentiation in a neuroblastoma cell line. Synaptobrevins/VAMPs, syntaxins, and the 25-kD synaptosomal-associated protein are the main components of a protein complex involved in the docking and/or fusion of vesicles and cell membranes. The VAMP5 gene is a member of the vesicle-associated membrane protein (VAMP)/synaptobrevin family and the SNARE superfamily. This VAMP family member may participate in vesicle trafficking events that are associated with myogenesis [70]. The significantly high expression of fam101b, Mag, cx47.1, cldnk and increase of VAMP5 genes in old zebrafish neural stem cells may be markers for newly generated neurons and crlf1a expression in old zebrafish stem cells indicates that the survival of neuronal cells is supported in order to make up for the loss caused by aging.

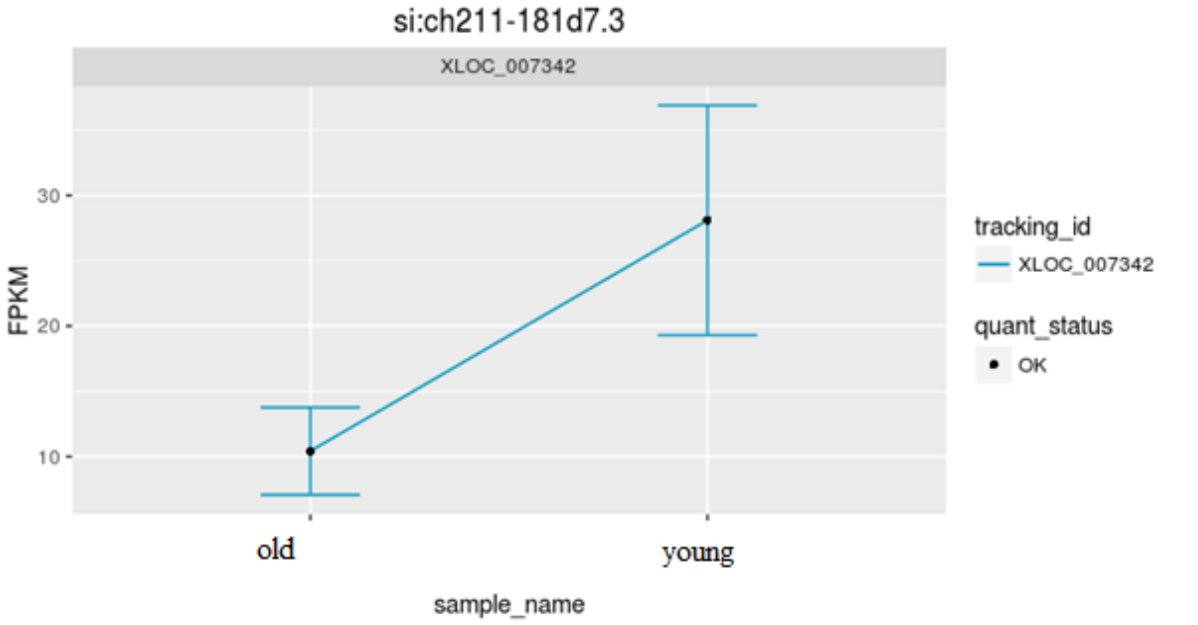

Figure 23: si:ch211-181d7.3 expression difference graph generated in R by cummeRbund package

RNA-seq analysis revealed that si:ch211-181d7.3 and Serpine1 are downregulated in old zebrafish neural stem cells whereas the other 16 differentially expressed genes were found to be upregulated compared to young zebrafish (Fig. 23). si:ch211-181d7.3 is a leucine-rich predicted protein. In a recent study, it was found that exposure of zebrafish to 17α-ethinylestradiol (EE2), an endocrine disrupting compound (EDC), caused increased anxiety and risky behaviors in adult zebrafish which indicated a neuroendocrine damage. The study analyzed RNA sequences obtained from exposed and unexposed fish which found that si:ch211-181d7.3 was upregulated (log fold change 0.99) in EDC exposed fish. The function of the gene remains elusive. No human ortholog have been reported [71].

Serpine1, plasminogen activator inhibitor-1 (PAT1), is a member of the serine proteinase inhibitor (serpin) superfamily. This member is the principal inhibitor of tissue plasminogen activator (tPA) and urokinase (uPA), and hence is an inhibitor of fibrinolysis. Serpine 1 expression is upregulated in age-related diseases such as Alzheimer's disease, cardiovascular diseases, diabetes mellitus and inflammation [72].

Normally, Serpine1 would be expected to have higher expression levels in old zebrafish brain stem cells compared to young zebrafish. However, Serpine1 is not only involved in age-related disorders, it is also involved in inflammation.

Contamination problems were encountered with young zebrafish while performing stem cell isolation. Doubling the amount of antibiotics used in the culture medium, which did not decrease the contamination level, also had a negative effect on the stem cells. Since C7 downregulation is linked to reduced levels of opsonization and neutrophil chemotaxis, the low levels of C7 in young zebrafish may indicate a problem with the immune system of the fish. Upregulation of si:ch211-181d7.3 in young fish may be linked to increased anxiety levels in zebrafish as it was shown in Eren, M *et al.*'s study [72]. Although it may or may not be related to a pathogen presence, the low levels of si:ch211-181d7.3 in old fish suggest that young fish are more stressed.

In a previous study conducted by Erbaba *et al.* (unpublished data), two zebrafish groups were compared for their RNA expression data. One group which received caloric restriction versus a normal fed control group was found to be expressing significant differences in the levels of serpine1, cx47.1, and si:ch211-181d7.3. cx47.1 and si:ch211-181d7.3 were upregulated in fish that were put on a caloric restriction regimen, potentially indicating an increase in anxiety and myelin formation. The increase in myelin formation might suggest an increase in neuron formation. Serpine1 upregulation in control group also suggests that control group, that received no caloric restriction, was aging faster.

The results show that most of the genes upregulated in the old zebrafish are involved in differentiation of neural stem cells and survival of neurons. This may suggest that the neural

stem cells of the young fish are in a quiescent state, which means that they are not differentiating or dividing. Whereas, the old zebrafish are in constant need of new neuron supply.

3.3.2 Immunocytochemistry

The difference in BrdU intake of old and young zebrafish did not show any significant difference in brain cell marker expressions (Begun Erbaba, unpublished data). However, due to the contamination in young zebrafish brain stem cell culture, the immunostaining results were obtained only from old zebrafish. The images were taken with Zeiss DIC equipped upright fluorescence microscope.

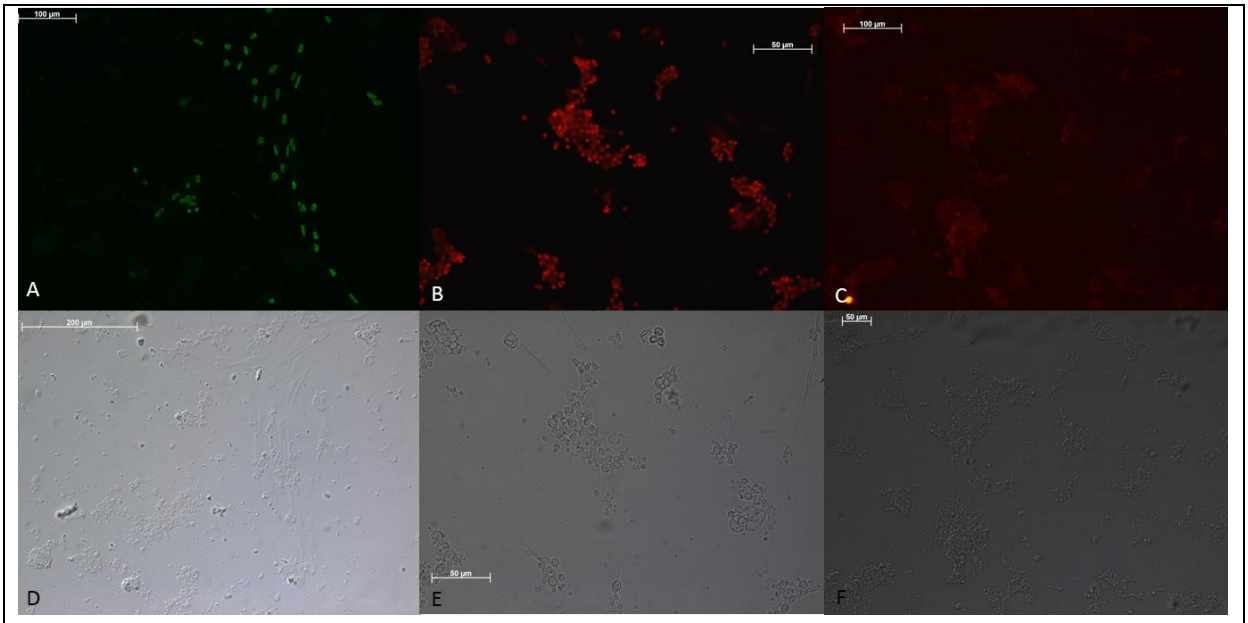

Figure 24: Immunostaining result of old zebrafish neural stem cells on non-coated slides. (a) BrdU staining, scale bar = 100 µm, (b) Islet staining, scale bar= 50 µm (c) NeuN staining, scale bar= 100 µm. (d), (e), (f) are taken with DIC filter. (a) and (d); (b) and (e), (c) and (f) show the same area.

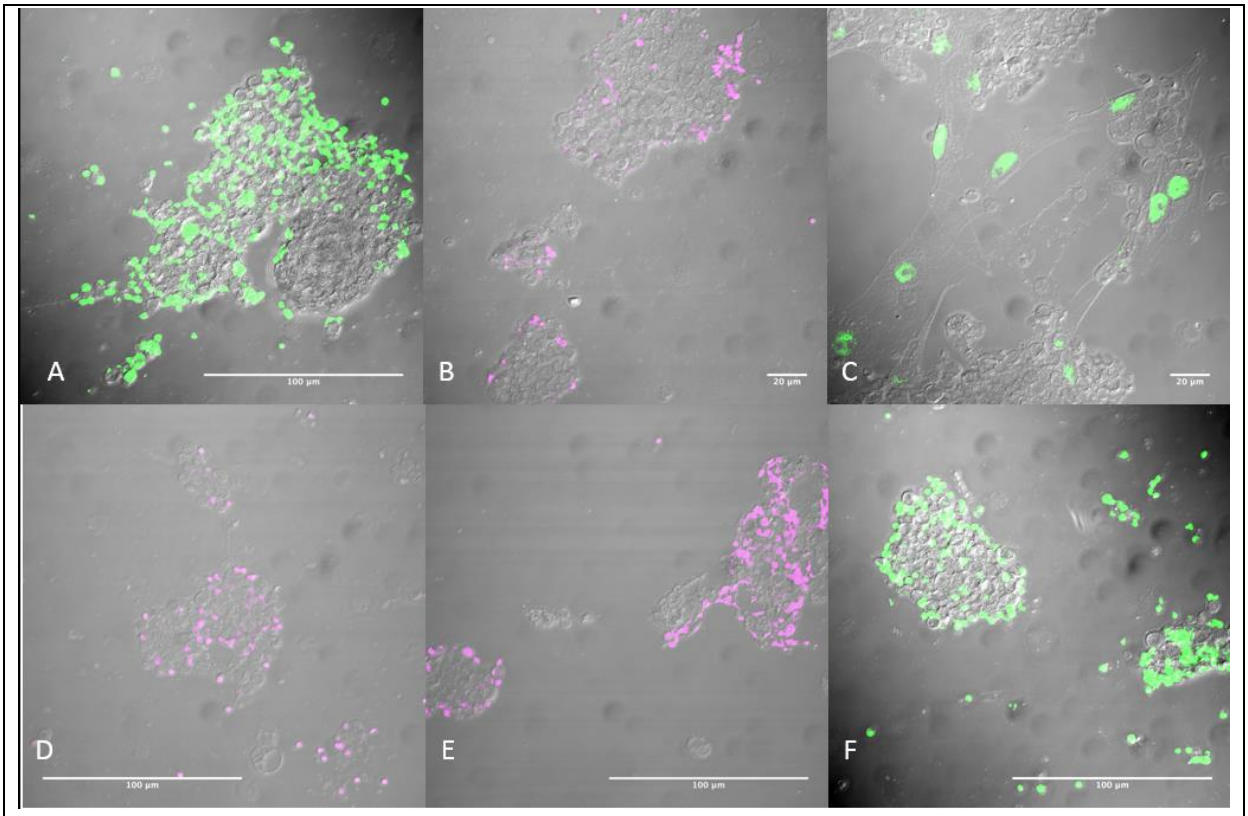

Figure 25: Immunostaining results of old zebrafish neural stem cells on non-coated slides. (a) Vimentin staining (green) overlapped with DIC image, scale bar =100 µm, (b) Sox2 staining overlapped with DIC image, scale bar = 20 µm, (c) PCNA staining overlapped with DIC image, scale bar= 20 µm, (d) NeuN staining overlapped with DIC image, scale bar= 100 µm (e) Islet staining overlapped with DIC image, scale bar= 100 µm, (f) Vimentin staining overlapped with DIC image, scale bar = 100 µm.

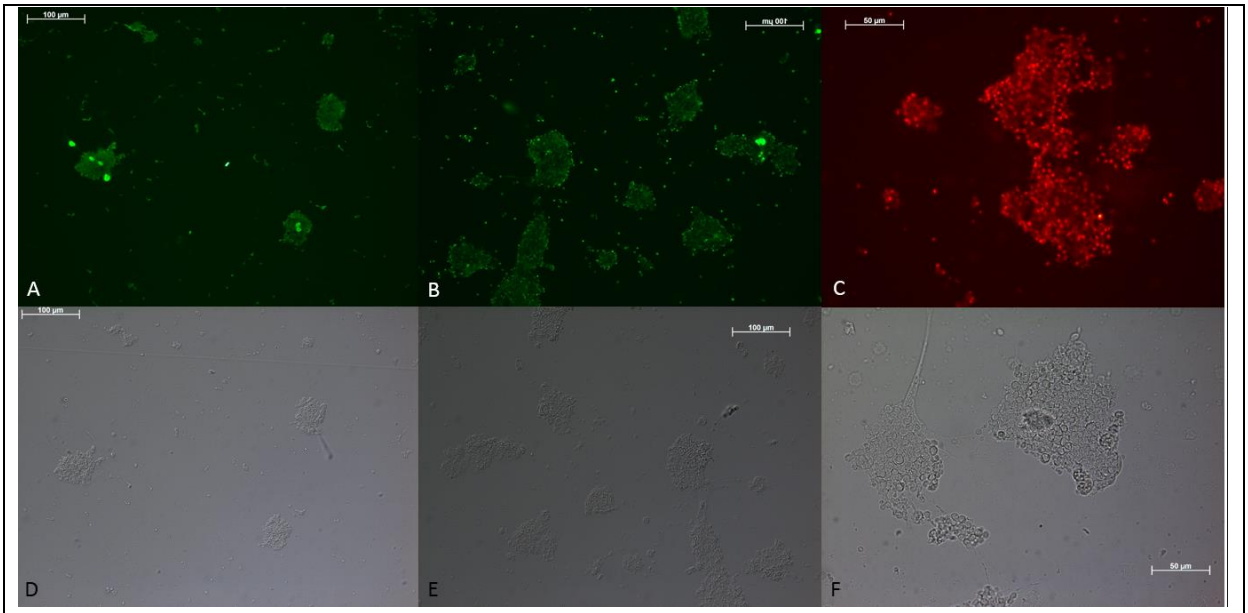

Figure 26: Immunostaining results of old zebrafish neural stem cells on Poly-L-lysine and laminin coated slides. (a) BrdU staining of the area in (d), scale bar= 100 µm, (b) BrdU staining, scale bar= 100 µm, (c) NeuN staining, scale bar = 50 µm. (d), (e) and (f) are taken with DIC filter.

Immunocytochemistry results demonstrate that the culture contains NeuN labeled neurons (Fig. 24c, 25d and 26c) as well as neural stem cells expressing Sox2 (Fig. 24b) and Islet-1 (Fig. 24b, 25e). Vimentin labeling (Fig. 25a) shows the localization of radial glial cells, which act as primary stem cells or progenitor cells. The results show that neural stem cells from zebrafish brain were successfully isolated and cultured. The culture is shown to contain both differentiated cells and stem cells in Figures 24c, 25d and 26c, as NeuN expression is a characteristic of mature neurons and Sox2 and Vimentin expressions (Figures 24 to 26) are stem cell markers.

3.4 CONCLUSION

The increased levels of genes responsible for neuron survival and regeneration in old zebrafish neural stem cells indicate that the stem cells are not only supporting the neural tissue by making new neurons or glial cells but also making gene products that support the neural cells' survival. In order to identify the genes' roles in RNA-seq results, the genes should be silenced and the resulting phenotypes should be investigated. The RNA-seq expression analysis should also be done with a larger sample space for the results to be more reliable and qPCR confirmation of the significantly differentially expressed genes should be carried out. For the functional inspection of the genes, genes will be knocked-out with morpholino injections.

CHAPTER 4

Cell Cycle Arrest and Flow Cytometry Analysis of C6 Cells

4.1 INTRODUCTION

Cancer is one of the leading causes of mortality worldwide and metastatic cancer is the cause of death in 9 of 10 cancer patients. Breast, colon and prostate cancers are the most common cancer types [73]. It is important to identify and quantify circulating tumor cells (CTCs) in blood for the diagnosis of cancer. The solid tumors of breast, colon and prostate cancer shed tumor cells into the blood stream. Hence CTC quantification can be valuable in monitoring the recovery period after chemotherapy, more accurate identification of the stage of cancer, and detecting relapse cases. Flow cytometry is a frequently used method for the enumeration and characterization of CTCs. However, cell characterization requires specific markers and no known marker is specific to CTCs [74].

Similar to stem cells, cancer cells are able to self-renew and proliferate. It is thought that cancer cells obtain the ability to proliferate indefinitely by gaining mutations that are necessary for malignancy. It is also known that cancers have their own supply of stem cells. Malignant gliomas contain glial and neuronal cells as well as undifferentiated cells. Cancer stem cells from different tumors divide slowly and are mostly quiescent (inactive) [75]. The fact that normal stem cells are resistant to chemotherapy has also been associated with the high expression of anti-apoptotic proteins and the excretion of chemotherapeutic drugs by the ATP-binding cassette (ABC) transporters. In FACS experiments, the excretion of Hoechst 33342 dye by the ABC transporters is used to isolate and form a subpopulation of tumor cells [76].

Glioblastomas are multivessel and lethal brain tumors. Inside, there are tumorigenic glioma stem cells (GSC) that are capable of self-renewal. GSCs are mostly located in the vein

surroundings. Identification of glioblastoma stem cells requires the use of multiple cell markers. In a study conducted by Trask *et al.*, it was observed that GSCs formed pericytes and supported tumor growth. It was also seen that the selective destruction of pericytes derived from GSC inhibits new vessel formation and tumor growth. GSCs were obtained from glioblastoma tumors and subjected to functional tests (self-renewal, multipotent, tumor formation, etc.). Alpha-SMA, NG2, CD248, and CD146 were used as pericyte markers. As a selective destruction method, GSCs were infected with the desmin-promoter-carrying herpes simplex virus thymidine kinase (HsvTK). HsvTK can metabolize ganciclovir, but it turns it into a toxic agent. Because they are only in G-pericytes, these cells can be selectively destroyed [77].

It was found that the C6 rat glioma cell line contains a subpopulation of cancer stem cells even after years in culture. The distinction between tumor cells and stem cells can be made using Hoechst 33342 exclusion [76]; and using a fluorescence-activated cell sorting (FACS) flow cytometer, the cells can be isolated and investigated further. Flow cytometry is used to count and analyze the size, shape, and properties of individual cells within a heterogeneous population of cells. The flow cytometer uses fluidics to move the samples into the flow cytometer, lasers, and light detectors. The flow cytometer mixes the cell suspension with a saline solution and leads the cells through a narrowing channel that causes the cells to form a single file line before they pass through the laser. Each cell is individually analyzed. As each cell passes through the laser beam, the beams scatter in multiple directions. The flow cytometer detects light scattered in a forward manner (FSCA) and light scattered in a sideways manner (SSCA). The amount of FSC is detected by a detector placed on the far size of the cell from the laser. FSC is proportional to the size of the cell. The detector converts the scattered light into a voltage pulse, which is directly proportional to the forward scattered light. The amount of side scattered light is detected by a detector located perpendicular to the path of the laser beam. SSC is proportional to the shape and internal complexity of a cell. The SSC is also converted into a voltage pulse.

By analyzing forward and side scattered data, a heterogeneous population of cells can be divided into individual populations with varying size shape and complexity [78]. Fig. 27 demonstrates the EM wave from a laser source hitting a cell and scattering of light. Flow cytometry can also be used to identify cell types with the help of cell marker specific antibodies linked to fluorochromes, as well as analyze the DNA content and cell viability [79].

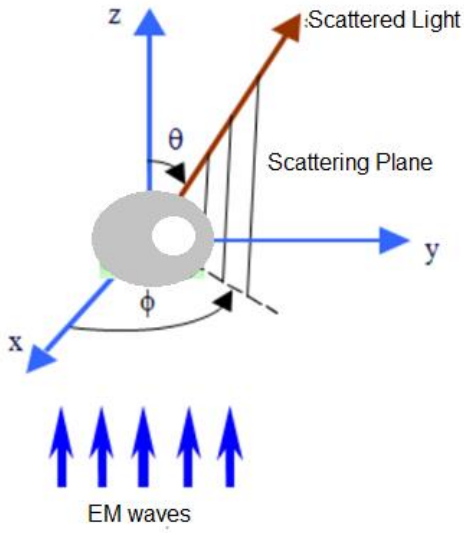

Figure 27: Depiction of a cell passing the laser beam inside the flow cytometer.

Early studies in flow cytometry have been limited in terms of the angle of incidence over which the scatter patterns are acquired. The cell morphology and the position of the cell when it hits the laser beam can cause significant variations in the 1-D scatter spectra. Collecting all the scattered light, and capturing 2-D scattering patterns would provide more information on the cells, and may allow the characterization of the cells [80].

Scattering cross section values of a cell provide essential information on its morphological properties. Thus, applications of the various optical detection technologies to the study of the components and morphological properties of cells have become one of the hot research topics. Scattering cross section values are critical evaluation criteria to diagnose the shape and the size parameters of the cell [81].

The eukaryote cell cycle goes through four stages: G1, S, G2 and M. In the G1 phase, the cell has n chromosomes, it is a gap phase and a pre-phase before the cell starts to replicate its DNA. The synthesis phase (S) is when the cell replicates its genetic material, it has more than n chromosomes but less than 2n chromosomes. G2 phase is also a gap phase where the decision to move on to M phase is made. In mitosis (M) phase, the cell divides. G1, S and G2 phases together are defined as interphase [82].

The goal of this study is to develop a method for the characterization of cells based on the angle resolved scattering patterns. Through this objective, measurements of the scattering cross section values (FSCA, SSCA) of cells from a C6 rat glioma cell line during the normal and arrested cell cycle were made. C6 cells are adherent and have a fibroblast-like morphology when attached to a surface. When in suspension, for flow cytometry measurements, the cells become sphere-like with a diameter of 8-10 microns [83]. The doubling time, the time spent for one cell cycle, of the C6 cells varies between 12-24 hours depending on the medium contents [96].

Another purpose is to identify scattering patterns specific to a cell line according to various morphology and characteristics throughout the normal cell cycle, generate a model for rat glioma cells and compare the scattering properties to healthy glial cells, and eventually eliminate the necessity for the use of markers in the routine identification processes.

4.2 METHODS

4.2.1 C6 Cells' handling

A C6 rat glioma cell line was received in frozen cryotubes (a gift from the Ayse Begum Tekinay group). The frozen samples were placed in a water bath in 37 ^{o}C and slowly shaken until

completely thawed. The vials were wiped with 70% ethanol to avoid contamination inside the hood. Since the cryoprotectant in the frozen samples was DMSO, the cells were washed with cell culture medium; 5 ml Penicillin-Streptomycin (15140-122, Gibco) and 50 ml fetal bovine serum (10270, Gibco) in 500 ml RPMI (21875-034, Gibco). They were centrifuged at 2000 RPM for 5 minutes at room temperature, the supernatant was aspirated, and the cell pellet was resuspended in 15 ml of cell culture medium and plated in an air vented T75 flasks. The flasks were placed in 37 ^{o}C incubator with the atmosphere inside consisting of 5% CO_2 and 95% air [84].

4.2.2 Passaging

When the cells reached 80% confluency the subculturing protocol was performed. The cells were washed with PBS (L0615-500, Biowest) twice, then treated with 0.25% Trypsin-EDTA (25200-056, Gibco) at 37 °C for 5 minutes. The trypsin was then inactivated with 10% FBS containing cell culture medium and the cell suspension and the cells were plated in 1:10 ratio diluted in cell culture medium. The remaining cell suspension was frozen and stored in liquid nitrogen tanks [85].

4.2.3 Cryopreservation

The cell suspension remaining from subculturing was centrifuged at 2000 RPM for 5 minutes, the supernatant was discarded and the pellet was resuspended in complete cell culture medium containing fetal bovine serum (10270, Gibco) and cell culture grade dimethylsulfoxide (A3272,0100; AppliChem) with a ratio of 8:1:1. The cells in cryopreservation media were then distributed into cryotubes and kept in Mr. Frosty (5100-0001, ThermoFisher) at -80 °C and transferred to liquid nitrogen tanks after a day.

4.2.4 Cell cycle arrest and determining the drug dosage

Once the cells reach 80% confluency, they were treated with different doses of nocodazole (M1404-2MG, Sigma) in order to find the minimum dosage required for cell cycle arrest at G2/M phase. Doses tested were 1µg/ml, 0.5 µg/ml, 0.25 µg/ml, 0.1 µg/ml and 0.05 µg/ml. The cells were treated with the specified concentrations of nocodazole and incubated at 37ºC for 24 hours [85].

4.2.5 Flow cytometry analysis

First, both nocodazole-treated and untreated cells were washed with PBS then treated with 0.25% Trypsin-EDTA for 5 minutes. The cells were washed with complete cell culture medium and centrifuged at 2000 RPM for 5 minutes. The supernatant was discarded and the cells were resuspended in PBS and centrifuged again at 2000 RPM for 5 minutes. After the supernatant was discarded the cells were fixed in cold 70% EtOH by dropwise adding while vortexing to avoid clumping of the cells. The cells were left in EtOH for 30 minutes on ice, then centrifuged at 2500 RPM and washed twice with PBS. The pellet was treated with 50 µl RNase A (Sigma) and 400 µl 1 µg/ml PI (P1304MP, Invitrogen) solution per million cells and resuspended in RNase and PI solution. The cells were incubated for 15 minutes at room temperature, then the cells' DNA content, forward and side scattering properties were measured with BD Accuri C6 flow cytometer [86].

4.3 RESULTS

4.3.1 Flow Cytometry

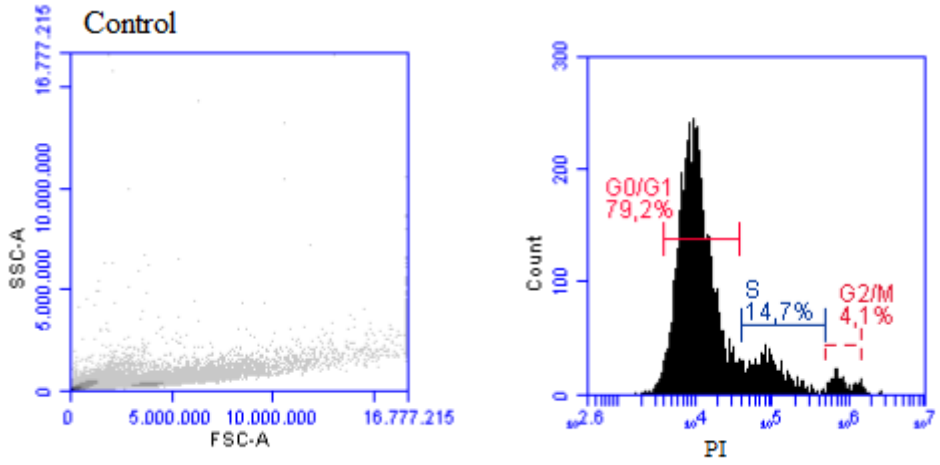

Figure 28: C6 cells' forward vs. side scatter and count vs. PI graph, no nocodazole treatment.

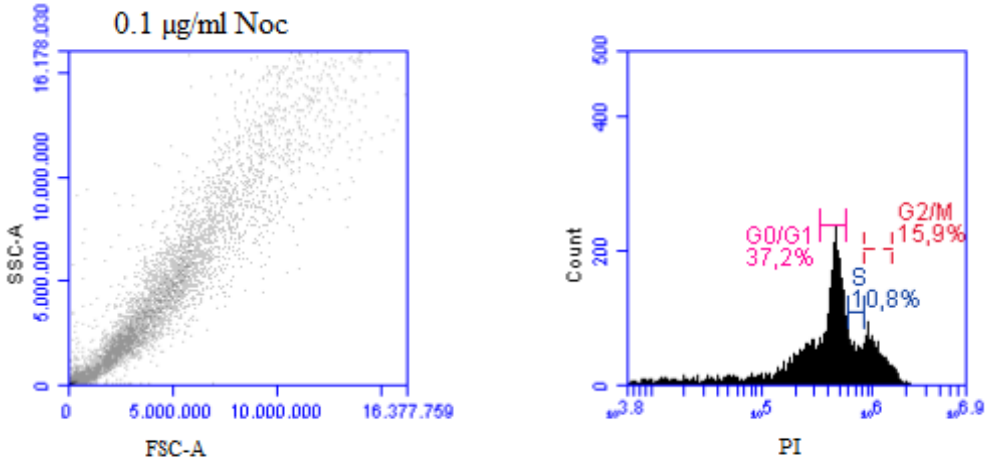

Figure 29: Forward and side scatter graph and count vs. PI graph of the 0.1 µg/ml nocodazole-treated C6 cells.

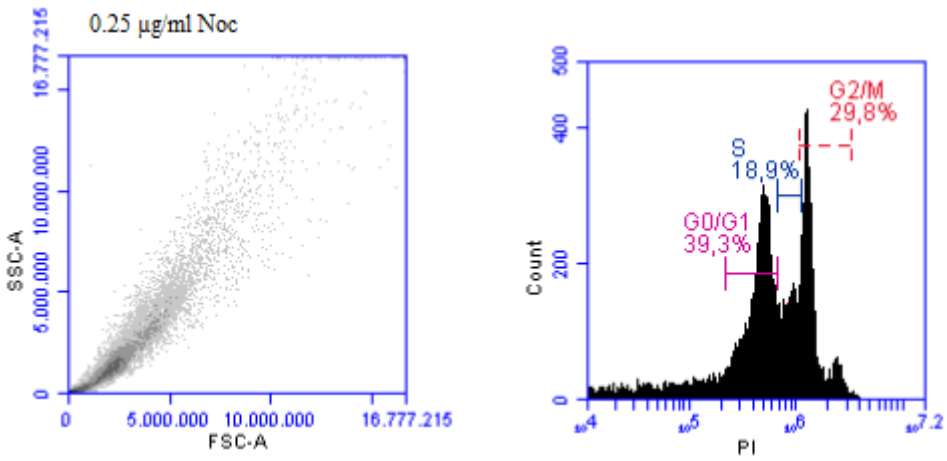

Figure 30: Forward and side scatter graph and count vs. PI graph of the 0.25 µg/ml nocodazole-treated C6 cells.

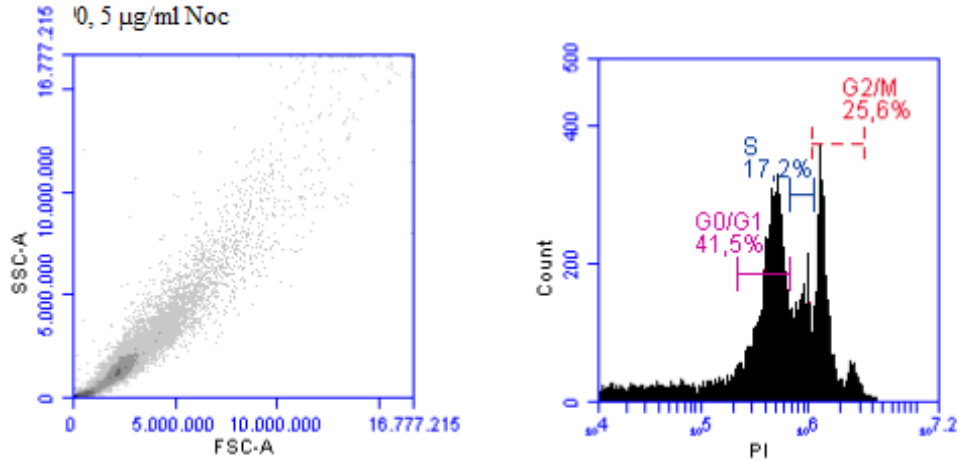

Figure 31: Forward and side scatter graph and count vs. PI graph of the 0.5 µg/ml nocodazole-treated C6 cells.

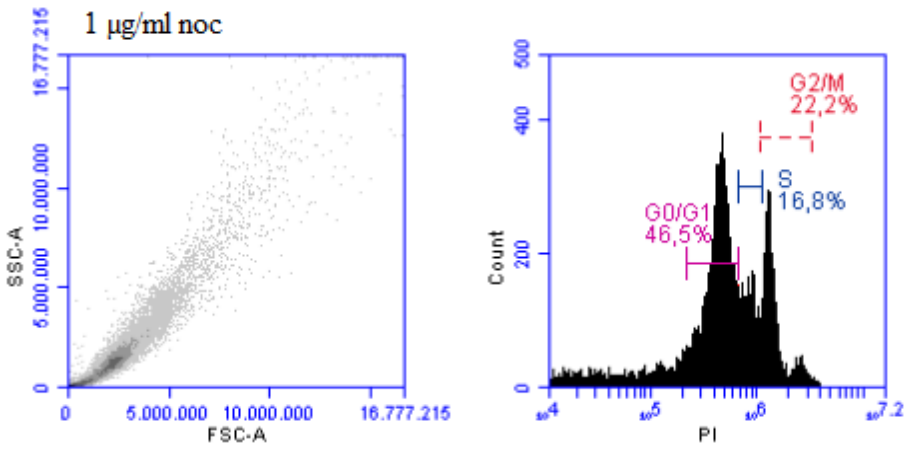

Figure 32: Forward and side scatter graph and count vs. PI graph of the 1 µg/ml nocodazole-treated C6 cells.

In Fig. 28, the C6 cells that received no nocodazole treatment had 4.1% of the total cell population in G2/M phase. This means that at a given time, only around 4% of the population was dividing. In figures 29-32, it was observed that the maximum percentage of cells in G2/M phase was in the condition when the cells were given 0.25 µg/ml nocodazole. The drug concentration was optimized and scattering cross section measurements were made in order to identify an interval for each phase of the cell. As cells grew and their granularity increased, the dots' (each representing a cell) side scatter and forward scattering values increased. When the cells divided, their FSC and SSC values went towards 0. PI stains DNA and the count vs. PI graph showed the genetic material changed, cells in G1 phase had n amount of genetic material, cells in the S phase had genetic material between n and 2n, and G2/M phase cells had 2n amount of genetic material, thus the signal increased or decreased depending on the amount of DNA.

4.3.2 Microscopy

The images were taken with Olympus IX53 inverted microscope.

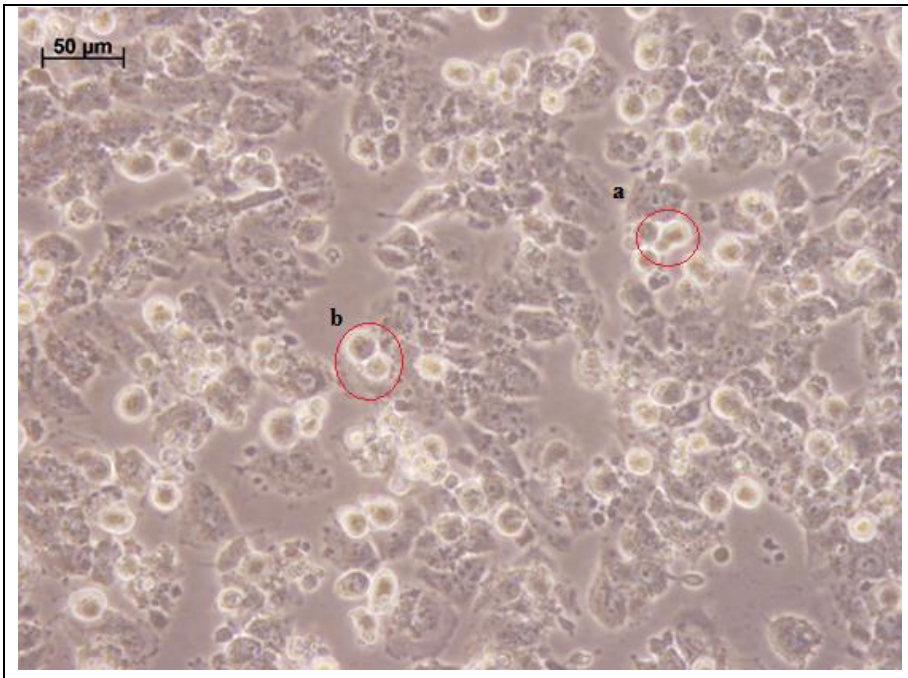

Figure 33: C6 cells after 24 hours of 0.25 µg/ml nocodazole treatment.

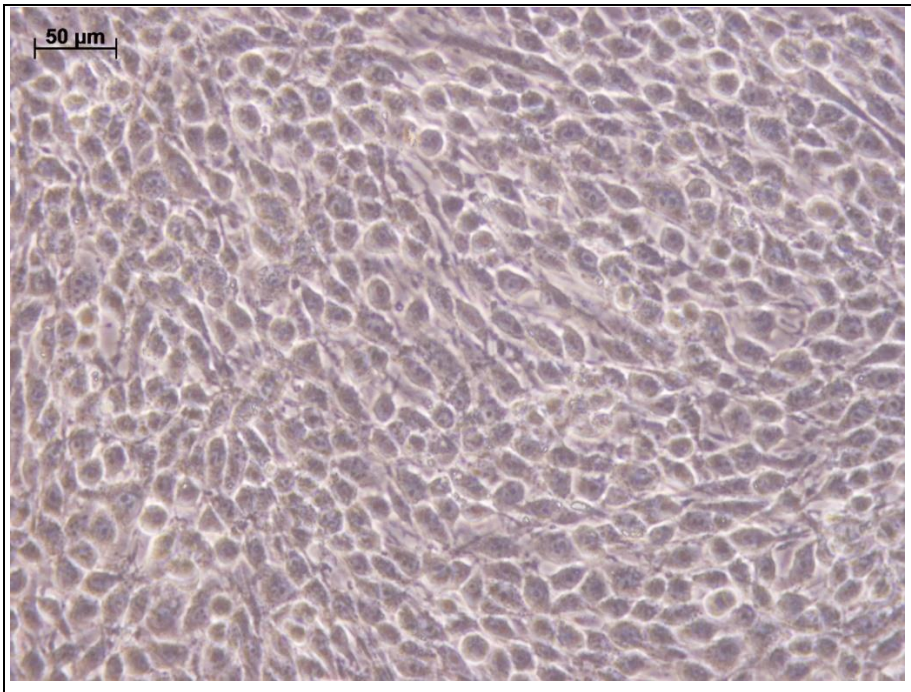

Figure 34: C6 cells with no nocodazole treatment.

Fig. 33 shows the C6 cells treated with 0.25 μg/ml nocodazole. It was observed that the cells arrested during G2/M phase were brighter than other cells. This might be due to the thinning of the cell membrane. Fig. 33 a shows a cell dividing the nucleus and b shows a cell dividing its membrane to make two separate daughter cells. Fig. 34 shows that C6 cells, indeed, have no contact inhibition. It is difficult to identify dividing cells since they make up around 4% of the population. Establishing a scattering interval based on the shape and internal complexity of certain cell types, different cell cycle phases, in this case, would serve as an identification for cells.

4.4 CONCLUSION

The C6 cells were successfully arrested at the G2/M phase and the nocodazole dosage was optimized. Future experiments should be conducted on human tumor cells in order to define an interval for diagnostic purposes. Cell markers can also be used in order to distinguish cancer stem cells and mature cancer cells in the C6 population. Flow cytometers have sorting properties, different types of cells can be grouped and analyzed separately for their scattering purposes. Defining scattering intervals for cells could help us distinguish different cell types in heterogeneous cell populations. The calculation and identification of scattering intervals for cells at different stages of the cell cycle were performed by Polat Goktas from Altintas group from the Electrical and Electronics Engineering Department of Bilkent University. Further studies will include the comparative study that will be conducted with healthy glial cells and tumorigenic glial cells in rats, and the identification of stem cells in tumor tissues based on their scattering properties.

CHAPTER 5

Conclusions and Future Perspectives

The studies have demonstrated that the cells isolated from tumor samples express proliferation and mature neuron markers, which may indicate the increased proliferation and growth rate of cancer stem cells. The expression analysis of zebrafish neural stem cells have shown that old zebrafish neural stem cells upregulate genes that have protective effects on mature neurons. Since cancer cells have a high rate of proliferation, the cell cycle was arrested for accurate monitoring of the cells in M phase and the ideal dosage was determined.

There is a need for the identification and isolation of cancer stem cells in order to characterize their cellular, physiological properties and drug resistance for the development of therapeutic agents. In this thesis project, the expression characteristics of human tumor stem cells and neural stem cells from old and young zebrafish were studied. Due to the differences in human tumor types, accurate marker expression differences could not be attributed to certain age groups (young and old). The ethical restrictions against obtaining healthy tissues from the patients in order to make a healthy and cancer stem cell marker expression comparison have caused the experiments to be done in a model organism.

The zebrafish was used in order to identify age-related expression differences in neural stem cells. A group of genes was found to be expressed differentially between old and young samples. In order to verify that the isolated cells were indeed stem cells, immunostaining experiments were carried out with specific neuronal and stem cell markers. The human tumor stem cell immunostaining results were more uniform, marker expression-wise compared to zebrafish neural stem cells. This may be attributed to the lack of EGF and FGF in culture mediums used for human tumor stem cells. As mentioned in the introduction, FGF and EGF keep the stem cells proliferating and decrease the differentiation rate. Thus, it can be seen that

in the neural stem cell staining of zebrafish, the proliferation marker expression is restricted to the outer cells of a colony. Whereas, almost all of the cells obtained from human tumors express proliferation markers. The results of zebrafish expression analysis demonstrated that the young zebrafish may have higher rates of anxiety and old fish have higher rates of stem cell differentiation and neuroprotective gene expression which can also be seen in the case of brain damage.

Finally, for the analysis of scattering properties of brain tumor cells (glioma cells), flow cytometry experiments were conducted. The cells were arrested at G2/M phase in order to define a scattering interval for the each cell cycle phase. Setting intervals for each cell type, would eliminate the use of biological markers and speed up the diagnosis process. The results of flow cytometry analysis, dosage optimization of chemotherapeutic agents and microscope images of G2 arrested and not arrested cells were shown. Stem cells have a great therapeutic potential with the drawback of the chance of having accumulated cancer-causing mutations. Thus, the identification of the differences between cancer and healthy stem cells is crucial. However, quiescent cancer stem cells are resistant to chemotherapy. Thus cancer stem cells should be directly targeted in therapy for definite results. It is known that cancer therapy affects healthy cells as well as cancer cells. Thus, a cell targeted therapy should be developed instead of destroying the local cells without the distinction of healthy or cancerous. The computer modeling of C6 cells is hoped to be a guide for the modeling of other disease causing cell modeling and identifications.

If the successful isolation and culture of healthy and cancer stem cells can be done, the computer modeling of cancer and normal stem cells could be a means of identification and monitoring cancer progression. With the help of sorting flow cytometers, the healthy stem cells in blood can be isolated, proliferated in a lab environment and given back to the patients in order to

increase the number of healthy cells and speed up recovery. Future studies are being planned to accomplish these aims.

Bibliography:

[1] A. Arslan-Ergul, A. Ozdemir, and M. Adams, "Aging, neurogenesis, and caloric restriction in different model organisms," *Aging Dis.*, vol. 4, no. 4, p. 221, 2013.

[2] O. Lazarov, M. Mattson, and D. Peterson, "When neurogenesis encounters aging and disease," *Trends Neurosci.*, vol. 33, no. 12, pp. 569–579, 2010.

[3] W. Deng, J. Aimone, and F. Gage, "New neurons and new memories: how does adult hippocampal neurogenesis affect learning and memory?," *Nat. Rev. Neurosci.*, vol. 11, no. 5, pp. 339–350, 2010.

[4] E. Gould, A. Beylin, P. Tanapat, and A. Reeves, "Learning enhances adult neurogenesis in the hippocampal formation," *Nat. Neurosci.*, vol. 2, no. 3, pp. 260–265, 1999.

[5] C. Zhao, W. Deng, and F. Gage, "Mechanisms and functional implications of adult neurogenesis," *Cell*, vol. 132, no. 4, pp. 645–660, 2008.

[6] A. Ernst and J. Frisén, "Adult neurogenesis in humans-common and unique traits in mammals," *PLoS Biol*, vol. 13, no. 1, p. e1002045, 2015.

[7] R. Chawana, N. Patzke, C. Kaswera, and E. Gilissen, "Adult neurogenesis in eight megachiropteran species," *Neuroscience*, vol. 244, pp. 159–172, 2013.

[8] N. Patzke, C. Kaswera, E. Gilissen, and A. Ihunwo, "Adult neurogenesis in a giant otter shrew (Potamogale velox)," *Neuroscience*, vol. 238, pp. 270–279, 2013.

[9] J. Campisi, "Aging, cellular senescence, and cancer," *Annu. Rev. Physiol.*, vol. 75, pp. 685–705, 2013.

[10] K. Jin, Y. Sun, L. Xie, S. Batteur, X. Mao, and C. Smelick, "Neurogenesis and aging:

FGF- 2 and HB- EGF restore neurogenesis in hippocampus and subventricular zone of aged mice," *Aging Cell*, vol. 2, no. 3, pp. 175–183, 2003.

[11] J. Luo, S. Daniels, J. Lennington, and R. Notti, "The aging neurogenic subventricular zone," *Aging Cell*, vol. 5, no. 2, pp. 139–152, 2006.

[12] H. Cameron and R. McKay, "Restoring production of hippocampal neurons in old age," *Nat. Neurosci.*, vol. 2, no. 10, pp. 894–897, 1999.

[13] G. Pan, Z. Chang, H. Schöler, and P. Duanqing, "Stem cell pluripotency and transcription factor Oct4," *Cell Res.*, vol. 12, no. 5, pp. 321–329, 2002.

[14] A. Bongso and M. Richards, "History and perspective of stem cell research," *Best Pract. Res. Clin. Obstet.*, vol. 18, no. 6, pp. 827–842, 2004.

[15] H. Kuhn, J. Winkler, and G. Kempermann, "Epidermal growth factor and fibroblast growth factor-2 have different effects on neural progenitors in the adult rat brain," *J.*, vol. 17, no. 15, pp. 5820–5829, 1997.

[16] A. Maslov, T. Barone, and R. Plunkett, "Neural stem cell detection, characterization, and age-related changes in the subventricular zone of mice," *J.*, vol. 24, no. 7, pp. 1726–1733, 2004.

[17] A. Gritti, P. Frölichsthal-Schoeller, and R. Galli, "Epidermal and fibroblast growth factors behave as mitogenic regulators for a single multipotent stem cell-like population from the subventricular region of the adult," *J.*, vol. 19, no. 9, pp. 3287–3297, 1999.

[18] V. Tabar and L. Studer, "Pluripotent stem cells in regenerative medicine: challenges and recent progress," *Nat. Rev. Genet.*, vol. 15, no. 2, pp. 82–92, 2014.

[19] R. Signer and S. Morrison, “Mechanisms that regulate stem cell aging and life span,” *Cell Stem Cell*, vol. 12, no. 2, pp. 152–165, 2013.

[20] L. Nguyen, R. Vanner, P. Dirks, and C. Eaves, “Cancer stem cells: an evolving concept,” *Nat. Rev. Cancer*, vol. 12, no. 2, pp. 133–143, 2012.

[21] T. Reya, S. Morrison, M. Clarke, and I. Weissman, “Stem cells, cancer, and cancer stem cells,” *Nature*, vol. 414, no. 6859, pp. 105–111, 2001.

[22] S. Singh, C. Hawkins, I. Clarke, J. Squire, and J. Bayani, “Identification of human brain tumour initiating cells,” *Nature*, vol. 432, no. 7015, pp. 396–401, 2004.

[23] D. Pattabiraman and R. Weinberg, “Tackling the cancer stem cells—what challenges do they pose?,” *Nat. Rev. Drug Discov.*, vol. 13, no. 7, pp. 497–512, 2014.

[24] S. Sell, “Stem cell origin of cancer and differentiation therapy,” *Crit. Rev. Oncol. Hematol.*, vol. 51, no. 1, pp. 1–28, 2004.

[25] M. Clarke, J. Dick, P. Dirks, and C. Eaves, “Cancer stem cells—perspectives on current status and future directions: AACR Workshop on cancer stem cells,” *Cancer Res.*, vol. 66, no. 19, pp. 9339–9344, 2006.

[26] F. Li, “Every single cell clones from cancer cell lines growing tumors in vivo may not invalidate the cancer stem cell concept,” *Mol. Cells*, vol. 27, no. 4, pp. 491–492, 2009.

[27] Z. Zhu, M. Khan, M. Weiler, J. Blaes, and L. Jestaedt, “Targeting self-renewal in high-grade brain tumors leads to loss of brain tumor stem cells and prolonged survival,” *Cell Stem Cell*, vol. 15, no. 2, pp. 185–198, 2014.

[28] R. Burrell, N. McGranahan, J. Bartek, and C. Swanton, “The causes and consequences of genetic heterogeneity in cancer evolution,” *Nature*, vol. 501, no. 7467, pp. 338–345,

2013.

[29] A. Kreso and J. Dick, “Evolution of the cancer stem cell model,” *Cell Stem Cell*, vol. 14, no. 3, pp. 275–291, 2014.

[30] J. Chen, Y. Li, T. Yu, R. McKay, D. Burns, and S. Kernie, “A restricted cell population propagates glioblastoma growth after chemotherapy,” *Nature*, vol. 488, no. 7412, pp. 522–526, 2012.

[31] P. Gupta, T. Onder, G. Jiang, K. Tao, and C. Kuperwasser, “Identification of selective inhibitors of cancer stem cells by high-throughput screening,” *Cell*, vol. 138, no. 4, pp. 645–659, 2009.

[32] Y. Zhu, F. Guignard, D. Zhao, L. Liu, D. Burns, and R. Mason, “Early inactivation of p53 tumor suppressor gene cooperating with NF1 loss induces malignant astrocytoma,” *Cancer Cell*, vol. 8, no. 2, pp. 119–130, 2005.

[33] E. Holland, J. Celestino, C. Dai, and L. Schaefer, “Combined activation of Ras and Akt in neural progenitors induces glioblastoma formation in mice,” *Nature*, vol. 25, no. 1, pp. 55–57, 2000.

[34] C. Dai, J. Celestino, Y. Okada, and D. Louis, “PDGF autocrine stimulation dedifferentiates cultured astrocytes and induces oligodendrogliomas and oligoastrocytomas from neural progenitors and astrocytes in vivo,” *Genes &*, vol. 15, no. 15, pp. 1913–1925, 2001.

[35] C. Tomasetti and B. Vogelstein, “Variation in cancer risk among tissues can be explained by the number of stem cell divisions,” *Science (80-.).*, vol. 347, no. 6217, pp. 78–81, 2015.

[36] Y. Begus-Nahrmann, A. Lechel, and A. Obenauf, “p53 deletion impairs clearance of chromosomal-instable stem cells in aging telomere-dysfunctional mice,” *Nature*, vol. 41, no. 10, pp. 1138–1143, 2009.

[37] K. Rudolph, S. Chang, H. Lee, M. Blasco, and G. Gottlieb, “Longevity, stress response, and cancer in aging telomerase-deficient mice,” *Cell*, vol. 96, no. 5, pp. 701–712, 1999.

[38] C. López-Otín, M. Blasco, L. Partridge, and M. Serrano, “The hallmarks of aging,” *Cell*, vol. 153, no. 6, pp. 1194–1217, 2013.

[39] D. Cornacchia and L. Studer, “Back and forth in time: Directing age in iPSC-derived lineages,” *Brain Res.*, vol. 1656, pp. 14–26, 2017.

[40] N. Kee, S. Sivalingam, and R. Boonstra, “The utility of Ki-67 and BrdU as proliferative markers of adult neurogenesis,” *J. Neurosci.*, vol. 115, no. 1, pp. 97–105, 2002.

[41] G. Dimri, X. Lee, G. Basile, and M. Acosta, “A biomarker that identifies senescent human cells in culture and in aging skin in vivo,” *Proc.*, vol. 92, no. 20, pp. 9363–9367, 1995.

[42] L. Schneider and F. d’Adda di Fagagna, “Neural stem cells exposed to BrdU lose their global DNA methylation and undergo astrocytic differentiation,” *Nucleic Acids Res.*, vol. 40, no. 12, pp. 5332–5342, 2012.

[43] S. Kishi, B. Slack, J. Uchiyama, and I. Zhdanova, “Zebrafish as a genetic model in biological and behavioral gerontology: where development meets aging in vertebrates–a mini-review,” *Gerontology*, vol. 55, no. 4, pp. 430–441, 2009.

[44] G. Gerhard, “Small laboratory fish as models for aging research,” *Ageing Res. Rev.*, vol. 6, no. 1, pp. 64–72, 2007.

[45] G. Lieschke and P. Currie, “Animal models of human disease: zebrafish swim into view,” *Nat. Rev. Genet.*, vol. 8, no. 5, pp. 353–367, 2007.

[46] K. Howe, M. Clark, C. Torroja, J. Torrance, and C. Berthelot, “The zebrafish reference genome sequence and its relationship to the human genome,” *Nature*, vol. 496, no. 7446, pp. 498–503, 2013.

[47] L. Yu, V. Tucci, S. Kishi, and I. Zhdanova, “Cognitive aging in zebrafish,” *PLoS One*, vol. 1, no. 1, p. e14, 2006.

[48] S. Kishi, P. Bayliss, J. Uchiyama, E. Koshimizu, and J. Qi, “The identification of zebrafish mutants showing alterations in senescence-associated biomarkers,” *PLoS*, vol. 4, no. 8, p. e1000152, 2008.

[49] M. Ozturk, A. Arslan-Ergul, S. Bagislar, and S. Senturk, “Senescence and immortality in hepatocellular carcinoma,” *Cancer Lett.*, vol. 286, no. 1, pp. 103–113, 2009.

[50] A. Arslan-Ergul and M. Adams, “Gene expression changes in aging zebrafish (Danio rerio) brains are sexually dimorphic,” *BMC Neurosci.*, vol. 15, no. 1, p. 29, 2014.

[51] A. Ergul, D. Halim, and M. Adams, “Bromodeoxyuridine (BrdU) labeling and immunohistochemical detection in adult zebrafish brain,” *Protoc Exch*, vol. 12, p. 23, 2013.

[52] K. Edelmann, L. Glashauser, and S. Sprungala, “Increased radial glia quiescence, decreased reactivation upon injury and unaltered neuroblast behavior underlie decreased neurogenesis in the aging zebrafish,” *J.*, vol. 521, no. 13, pp. 3099–3115,

2013.

[53] R. Schmidt, U. Strähle, and S. Scholpp, “Neurogenesis in zebrafish–from embryo to adult,” *Neural*, vol. 8, no. 1, p. 3, 2013.

[54] M. Rao and M. Mattson, “Stem cells and aging: expanding the possibilities,” *Mech. Ageing Dev.*, vol. 122, no. 7, pp. 713–734, 2001.

[55] A. Tapanes-Castillo, F. Shabazz, and M. Mboge, “Characterization of a novel primary culture system of adult zebrafish brainstem cells,” *J. Neurosci.*, vol. 223, pp. 11–19, 2014.

[56] A. Yates, W. Akanni, M. Amode, and D. Barrell, “Ensembl 2016,” *Nucleic acids*, 2015.

[57] C. Trapnell, A. Roberts, L. Goff, G. Pertea, and D. Kim, “Differential gene and transcript expression analysis of RNA-seq experiments with TopHat and Cufflinks,” *Nat. Protoc.*, vol. 7, no. 3, pp. 562–578, 2012.

[58] T. Hayakawa, Y. Nagai, E. Nohara, and H. Yamashita, “Variation of the fatty acid binding protein 2 gene is not associated with obesity and insulin resistance in Japanese subjects,” *Metabolism*, vol. 48, no. 5, pp. 655–657, 1999.

[59] D. Deutsch, E. Fermon, J. Lustmann, and L. Dafni, “Tuftelin mRNA is expressed in a human ameloblastoma tumor,” *Connect. tissue*, vol. 39, no. 1–3, pp. 177–184, 1998.

[60] F. Vázquez-Chona and B. Song, “Temporal changes in gene expression after injury in the rat retina,” *Invest. Ophthalmol. Vis. Sci.*, vol. 45, no. 8, pp. 2737–2746, 2004.

[61] G. Stepanov, J. Filippova, and A. Komissarov, “Regulatory role of small nucleolar RNAs in human diseases,” *BioMed Res.*, vol. 2015, 2015.

[62] A. Bosio, E. Binczek, M. Le Beau, A. Fernald, and W. Stoffel, “The human gene CGT encoding the UDP-galactose ceramide galactosyl transferase (cerebroside synthase): cloning, characterization, and assignment to human,” *Genomics*, vol. 34, no. 1, pp. 69–75, 1996.

[63] X. Yin, T. Crawford, J. Griffin, and P. Tu, “Myelin-associated glycoprotein is a myelin signal that modulates the caliber of myelinated axons,” *J.*, vol. 18, no. 6, pp. 1953–1962, 1998.

[64] D. Menichella and D. Goodenough, “Connexins are critical for normal myelination in the CNS,” *J.*, vol. 23, no. 13, pp. 5963–5973, 2003.

[65] H. Cosar, Z. Kahramaner, and A. Erdemir, “Homozygous mutation of CRLF-1 gene in a Turkish newborn with Crisponi syndrome,” *Clin. dysnorphology*, vol. 20, no. 4, pp. 187–189, 2011.

[66] M. Naughton, M. Walport, and R. Würzner, “Organ-specific contribution to circulating C7 levels by the bone marrow and liver in humans,” *Eur. J.*, vol. 26, no. 9, pp. 2108–2112, 1996.

[67] R. Oka, T. Sasagawa, I. Ninomiya, K. Miwa, and H. Tanii, “Reduction in the local expression of complement component 6 (C6) and 7 (C7) mRNAs in oesophageal carcinoma,” *Eur. J.*, vol. 37, no. 9, pp. 1158–1165, 2001.

[68] C. Papanayotou, I. De Almeida, and P. Liao, “Calfacilitin is a calcium channel modulator essential for initiation of neural plate development,” *Nature*, vol. 4, p. 1837, 2013.

[69] E. Münzel, K. Schaefer, B. Obirei, and E. Kremmer, “Claudin k is specifically expressed in cells that form myelin during development of the nervous system and

regeneration of the optic nerve in adult zebrafish," *Glia*, vol. 60, no. 2, pp. 253–270, 2012.

[70] J. Sørensen, "SNARE complexes prepare for membrane fusion," *Trends Neurosci.*, vol. 28, no. 9, pp. 453–455, 2005.

[71] T. Porseryd, K. Volkova, and N. Caspillo, "Persistent effects of developmental exposure to 17α-ethinylestradiol on the zebrafish (Danio rerio) brain transcriptome and behavior," *Front.*, vol. 11, 2017.

[72] M. Eren, A. Boe, and E. Klyachko, "Role of plasminogen activator inhibitor-1 in senescence and aging," *Semin. Thromb.*, vol. 40, no. 6, pp. 645–651, 2014.

[73] R. L. Siegel, K. D. Miller, and A. Jemal, "Cancer statistics, 2017," *CA. Cancer J. Clin.*, vol. 67, no. 1, pp. 7–30, Jan. 2017.

[74] J. De Bono, H. Scher, R. Montgomery, and C. Parker, "Circulating tumor cells predict survival benefit from treatment in metastatic castration-resistant prostate cancer," *Clin. Cancer*, vol. 14, no. 19, pp. 6302–6309, 2008.

[75] S. Pece, D. Tosoni, S. Confalonieri, and G. Mazzarol, "Biological and molecular heterogeneity of breast cancers correlates with their cancer stem cell content," *Cell*, vol. 140, no. 1, pp. 62–73, 2010.

[76] T. Kondo, T. Setoguchi, and T. Taga, "Persistence of a small subpopulation of cancer stem-like cells in the C6 glioma cell line," *Proc. Natl.*, vol. 101, no. 3, pp. 781–786, 2004.

[77] T. Trask, R. Trask, E. Aguilar-Cordova, and H. Shine, "Phase I study of adenoviral delivery of the HSV-tk gene and ganciclovir administration in patients with recurrent

malignant brain tumors," *Mol. Ther.*, vol. 1, no. 2, pp. 195–203, 2000.

[78] "BD Accuri™ C6 | Flow Cytometer | BD Biosciences." [Online]. Available: http://www.bdbiosciences.com/instruments/accuri/. [Accessed: 19-Jun-2017].

[79] I. Nicoletti, G. Migliorati, M. Pagliacci, and F. Grignani, "A rapid and simple method for measuring thymocyte apoptosis by propidium iodide staining and flow cytometry," *J.*, vol. 139, no. 2, pp. 271–279, 1991.

[80] X. Su, C. Capjack, W. Rozmus, and C. Backhouse, "2D light scattering patterns of mitochondria in single cells," *Opt. Express*, vol. 15, no. 17, pp. 10562–10575, 2007.

[81] R. Brown, "Absorption and scattering of light by small particles," *J. Mod. Opt.*, vol. 31, no. 1, p. 3, 1984.

[82] S. Elledge, "Cell cycle checkpoints: preventing an identity crisis," *Science (80-.).*, vol. 274, no. 5293, p. 1664, 1996.

[83] T. Wan, W. Pan, Y. Long, K. Yu, and S. Liu, "effects of nanoparticles with hydrotropic nicotinamide on tacrolimus: permeability through psoriatic skin and antipsoriatic and antiproliferative activities," *Int. J.*, vol. 12, p. 1485, 2017.

[84] T. Okabe, N. Sato, Y. Kondo, S. Asano, and N. Ohsawa, "Establishment and characterization of a human cancer cell line that produces human colony-stimulating factor," *Cancer Res.*, vol. 38, no. 11, pp. 3910–3917, 1978.

[85] K. Kato, H. Ito, Y. Inaguma, K. Okamoto, and S. Saga, "Synthesis and accumulation of αB crystallin in C6 glioma cells is induced by agents that promote the disassembly of microtubules," *J. Biol.*, vol. 271, no. 43, pp. 26989–26994, 1996.

[86] G. Cinar, A. Ozdemir, S. Hamsici, G. Gunay, and A. Dana, "Local delivery of

doxorubicin through supramolecular peptide amphiphile nanofiber gels," *Biomaterials*, vol. 5, no. 1, pp. 67–76, 2017.

Appendix A

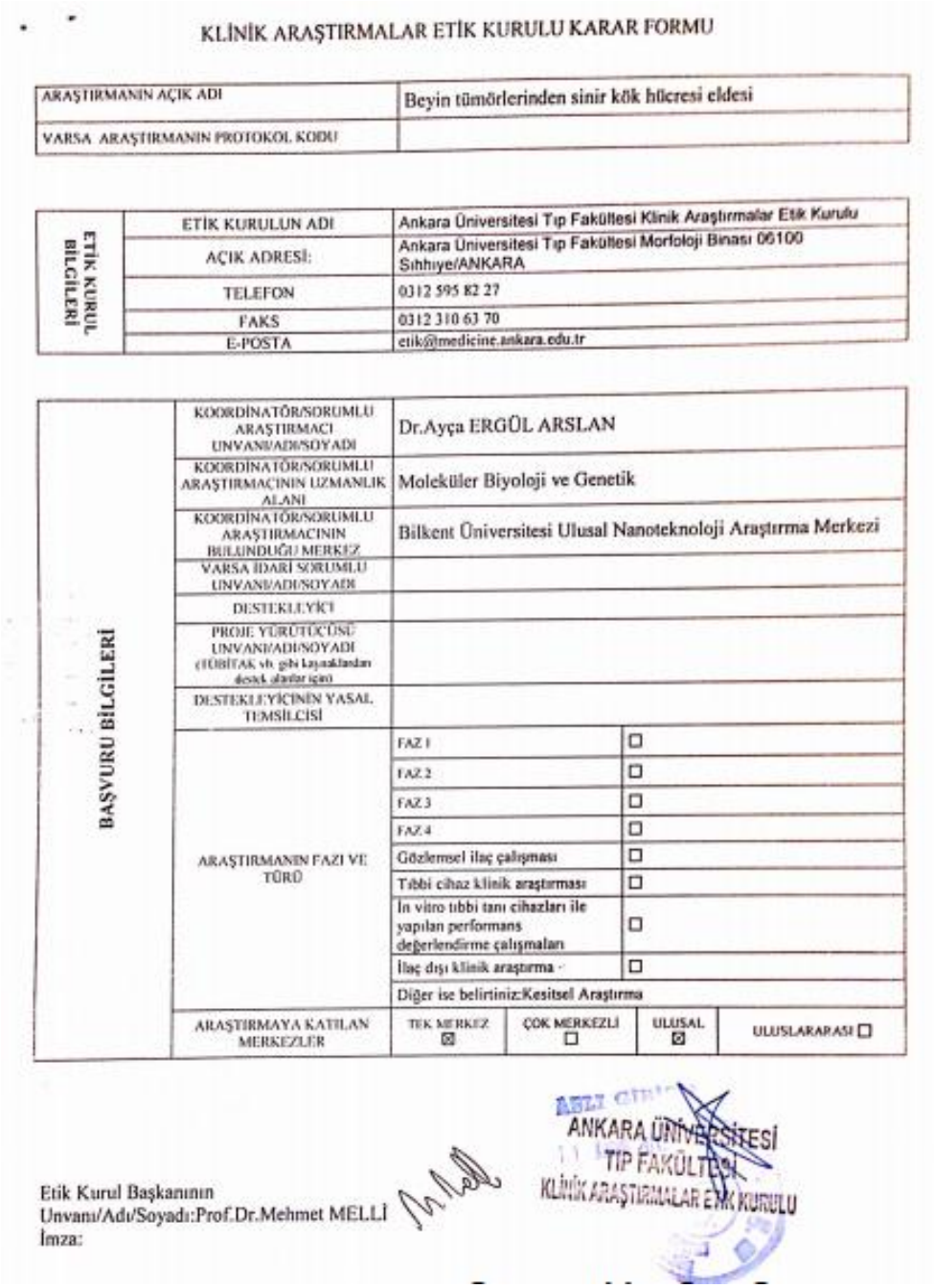

KLİNİK ARAŞTIRMALAR ETİK KURULU KARAR FORMU

ARAŞTIRMANIN AÇIK ADI	Beyin tümörlerinden sinir kök hücresi eldesi
VARSA ARAŞTIRMANIN PROTOKOL KODU	

ETİK KURUL BİLGİLERİ	ETİK KURULUN ADI	Ankara Üniversitesi Tıp Fakültesi Klinik Araştırmalar Etik Kurulu
	AÇIK ADRESİ:	Ankara Üniversitesi Tıp Fakültesi Morfoloji Binası 06100 Sıhhiye/ANKARA
	TELEFON	0312 595 82 27
	FAKS	0312 310 63 70
	E-POSTA	etik@medicine.ankara.edu.tr

BAŞVURU BİLGİLERİ	KOORDİNATÖR/SORUMLU ARAŞTIRMACI UNVANI/ADI/SOYADI	Dr.Ayça ERGÜL ARSLAN			
	KOORDİNATÖR/SORUMLU ARAŞTIRMACININ UZMANLIK ALANI	Moleküler Biyoloji ve Genetik			
	KOORDİNATÖR/SORUMLU ARAŞTIRMACININ BULUNDUĞU MERKEZ	Bilkent Üniversitesi Ulusal Nanoteknoloji Araştırma Merkezi			
	VARSA İDARİ SORUMLU UNVANI/ADI/SOYADI				
	DESTEKLEYİCİ				
	PROJE YÜRÜTÜCÜSÜ UNVANI/ADI/SOYADI (TÜBİTAK vb. gibi kuruluşlardan destek alanlar için)				
	DESTEKLEYİCİNİN YASAL TEMSİLCİSİ				
	ARAŞTIRMANIN FAZI VE TÜRÜ	FAZ 1	☐		
		FAZ 2	☐		
		FAZ 3	☐		
		FAZ 4	☐		
		Gözlemsel ilaç çalışması	☐		
		Tıbbi cihaz klinik araştırması	☐		
		İn vitro tıbbi tanı cihazları ile yapılan performans değerlendirme çalışmaları	☐		
		İlaç dışı klinik araştırma	☐		
		Diğer ise belirtiniz:Kesitsel Araştırma			
	ARAŞTIRMAYA KATILAN MERKEZLER	TEK MERKEZ ☒	ÇOK MERKEZLİ ☐	ULUSAL ☒	ULUSLARARASI ☐

Etik Kurul Başkanının
Unvanı/Adı/Soyadı:Prof.Dr.Mehmet MELLİ
İmza:

ANKARA ÜNİVERSİTESİ
TIP FAKÜLTESİ
KLİNİK ARAŞTIRMALAR ETİK KURULU

Appendix B

BİLKENT ÜNİVERSİTESİ HAYVAN DENEYLERİ ETİK KURUL KARARI

TOPLANTI TARİH : 24.3.2014
TOPLANTI NO : 2
DOSYA NO : 18
KARAR NO : 2014/18

Dr. Ayça Arslan Ergül'ün "Yaşlanan zebrabalığı beyninden kök hücre eldesi" başlıklı araştırma deney protokolü Hayvan Deneyleri Etik Kurulu'nda incelenmiş, yapılan inceleme sonucunda çalışmanın Hayvanları Deneyleri Etik Kurulu Yönergesi'ne göre uygun bulunarak onaylanmasına katılan üyelerin oy birliği ile karar verilmiştir.

İhsan Gürsel (Başkan)

Ergin Atalar (Üye)

Michelle Adams (Üye)

Z. Gamze Aykut (Üye)

Ahmet Raşit Öztürk (Üye)

Teoman König (Üye)

Appendix C

Isolation, Manipulation and Transplantation of Aged Zebrafish Brain Stem Cells

Begün Erbaba[1], Özge Burhan[1], Esra Şenol[2], Nazlı Akıllı[2], Michelle M. Adams[1,3], Ayça Arslan Ergül[4]

[1] Bilkent University, Interdisciplinary Program of Neuroscience
[2] Bilkent University, Department of Molecular Biology and Genetics
[3] Bilkent University , Department of Psychology
[4] Hacettepe University, Transgenic Animal Technologies R.A.C.
06800 Ankara, Turkey

Introduction

As nature dictates, aging is inevitable for humans. Like our bodies, our brains also get older and lose cognitive abilities. The brain is composed of various types of cells including neurons, glia, and stem cells, which are the dividing cells that can give rise to either neurons or glia, and are thought to be affected in aging processes. With the help of these stem cells, our brains are capable of regenerating at all ages with a decreasing rate as the organism grows older. We formed our hypothesis around the following; since old individuals have old stem cells that are taking part in neurogenesis at a lower rate than their younger counterparts, then we may find a way to make the old ones young again if we can determine the differences between old and young derived stem cells. For our purpose we used zebrafish as model organism due to its advantages in terms of its handy complete brain size, graduate aging process like mammals do, and highly regenerative capabilities as compared to mammals.

Conclusions

The preliminary findings of our study demonstrate that we have successfully isolated neural cells from whole zebrafish brains with the current protocols, and found that 33 significant differentially expressed aging-related genes, such as *Serpine 1*, in brain stem cells. Aiming to present a method that can prevent cognitive aging, we believe that our project will shed light on the relationship between neurogenesis & stem cells in the old brain and their link to most of the age-related diseases. We will further confirm these genes by increasing the sample size and investigate their effects on phenotypes in future experiments.

This project is supported by TUBITAK Grant (114S548) of Ayça Arslan Ergül. We would like to thank Christos Papadimitriou from Çağhan Kızıl Lab, DZNE Dresden, for their help in developing a properly working protocol for neural stem cell isolation from the zebrafish brain, and Furkan Akdemir and Fatma Kahveci for their support with data analysis.

Methods

Maintanence of the Animals

Wild-type AB strain, young (8-9 month) and old (25-28 month) zebrafish were used. Animals were fed twice a day with dry food and three times a week with artemia and kept in standard conditions.

Neural Stem Cell Isolation and Culturing

After anesthesizing and decapitating the animals, brains were dissected and underwent a stem cell isolation procedure using MACS Miltenyi Biotec Neural Tissue Dissociation Kit(P). Isolated stem cells were seeded using L15 medium (supplemented with 1% P/S, 5%FBS, 20ng/ml EGF & FGF) onto the poly-D Lysin and Laminin coated culture plates (for ICC), 75cm^2 Corning Cell Bind flasks (for RNA Seq.), or Falcon™ Chambered Cell Culture Slides (for ICC) and were incubated at 28°C. Five to ten fish brains were pooled prior to the stem cell isolation procedure depending on the size of the culture area, in order to obtain a visible amount of stem cells in a culture.

Immunocytochemistry

For immunocytochemistry (ICC) experiments, we optimized a previous protocol adjusted for immunohistochemistry specifically for zebrafish brain. The cells on the slides were fixed with previously cooled MeOH (+4°C) for 1h, washed with PBS-T (PBS with 0.5% Tween), then treated with 2N HCl for 10 min., neutralized with borax buffer, and blocked with 3% goat serum for 1h. After a 1,5h incubation of the primary antibodies (anti- SOX2/ Vimentin/ BLBP/ islet/ GFAP/ NeuN/ GABA/ PSD95/ PCNA/ BrdU, Tau), a 1h secondary antibody (anti-mouse Alexa Fluor 488, anti-rabbit 555) incubation was performed. An additional 4h incubation with BrdU was performed prior to ICC for BrdU Ab. stainings. We used Invitrogen Prolong antifade reagent at the end to prevent signal loss. We utilized both a Zeiss fluorescence and LSM 510 confocal microscopes for visualization.

RNA Sequencing

After anesthesia and decapitation, whole fish brains were dissected under the stereo microscope. Total RNAs were isolated from the scraped stem cell cultures, each containing 10 fish brain isolates, using Qiagen's RNeasy Mini Kit according to the manufacturer's instructions. The isolation protocol was followed by DNase treatment with Ambion TURBO DNA-free Kit from Thermo Fisher Scientific. The resulting RNA samples were processed and sequenced at TUBITAK-MAM (by service procurement) with Illumina RNA Sequencing Technology. After obtaining the .fastq files, we analyzed the initial data coming from the RNA sequencing of the young and old fish brain stem cell cultures (20 fish).

The FastQC tool was used for the quality analysis of the Illumina RNA-seq reads, Bowtie2 was for building an index for zebrafish, Tophat2 for the alignment of the reads to the index file, Cufflinks for assembling the transcripts, Cuffmerge to merge the transcripts, Cuffquant for the quantification of the transcripts, Cuffdiff to compare the expression levels of samples and lastly cummeRbund was used to visualize the data.

Further Protocols

Currently, we are at the level of the RNA sequencing step of our experiments. Next, upon a selection of promising genes, we will proceed with knock-down & upregulation approaches for the old stem cells inversely depending on their behavior with advancing age. For this part, right now we are also optimising the protocols for morpholino (compound designed to prevent a gene of interest from being turned on in the developing embryo) and mRNA injections (to study the effect of too much gene expression) to zebrafish embryo and adults. Finally, we hope to perform transplantation experiments to replace the old and uneffective stem cells with their treated versions for the sake of rejuvenation.

Results

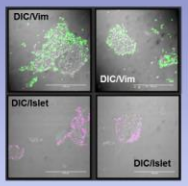

Positive signals of Vimentin antibody in the immunostaining of neural stem cell cultures merged with DIC filter (63x). Vimentin is an intermediate filament protein mainly exhibited in the radial-glial cells which are primary progenitors of CNS. It is not or rarely expressed in postmitotic neurons.

Positive signals of Islet antibody in the immunostaining of neural stem cell cultures merged with DIC filter (63x). Islet 1 and 2 are expressed in motor neuron progenitors.

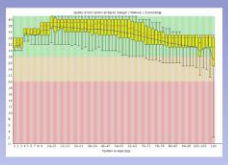

FASTQC Quality score of one of the preliminary data coming from high throughput RNA sequencing of 2 samples (old and young fish brain derived neural cell cultures that are obtained from 10 pooled brains for each).

Results coming from cuffdiff output using CummeRbund package of R (sbgenomics) shows some information such as number of samples, genes, isoforms, etc.

Heatmap of the genes showing significant differential expression (p≤0.05). Data obtained from cuffdiff output loaded to CummeRbund.

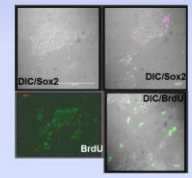

Positive signals of Sox2 antibody in the immunostaining of neural stem cell cultures merged with DIC filter (63x). Sox2 is found in undifferentiated neuronal progenitors. The signals were seen specifically at the edges of neuronal colonies. This finding was in accordance with BrdU stainings (40x / 63x) which is a marker for cell proliferation.

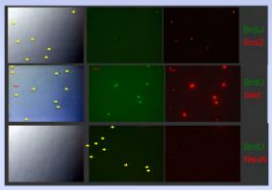

Double immunostaining signals from neural stem cell cultures . Left: DIC, Middle: BrdU, Right: Antibody for Sox2/Islet1/NeuN (BrdU/Sox2: 40x, BrdU/Islet1: 100x, BrdU/NeuN: 40x). The initial findings with the BrdU/Sox2 stainings showed that all cells were positive for both BrdU and Sox2; BrdU/Islet1 stainings showed that some cells expressing islet1 protein were negative for BrdU, and some cells were negative for both antibodies; and BrdU/NeuN stainings showed no NeuN signal.

Our preliminary results point 33 differentially expressed genes between old and young fish brain derived neural cell cultures from Cuffdiff results of RNA Sequencing data.

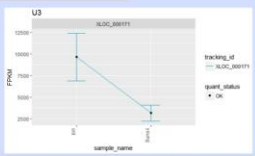

Expression data based on different parameters can be plotted individually for each gene. Diagram on the right isone of the plots and it presents U3 gene expression difference between samples according to fragments per kilobase of exon per million fragments mapped.

Appendix D

Leiden University Medical Center

BioSB research school

CERTIFICATE OF PARTICIPATION

This is to confirm that:

Özge Pelin Burhan

has attended the BioSB course:

RNA-seq data analysis (6th edition)

which was held on **September 26 - 28 2016**
at the **LUMC, Leiden, The Netherlands**

This course was organized by the BioSB research school together with the Leiden University Medical Center (LUMC).

This advanced 3-day course for people with experience in NGS consisted of seminars and hands-on command line, Galaxy and R practicals and covered the analysis pipelines for differential transcript expression and variant calling.

28 September 2016

Dr. Peter-Bram 't Hoen
Associate Professor
Leiden University Medical Center
Course Coordinator

Dr. Jan Oosting
Assistant Professor
Leiden University Medical Center
Course Coordinator

BioSB research school
Geert Grooteplein 28 (route 260), 6525 GA Nijmegen, The Netherlands
T: +31 (0)24 3619500, E: education@biosb.nl, W: www.biosb.nl